LA-UR-16-24559
Approved for public release; distribution is unlimited.

Title: On the velocity dependence of the dislocation drag coefficient from phonon wind

Author(s): Blaschke, Daniel
Mottola, Emil
Preston, Dean Laverne

Intended for: Report
Web

Issued: 2018-05-29 (rev.4)

LA-UR-16-24559

On the velocity dependence of the dislocation drag coefficient from phonon wind

Daniel N. Blaschke, Emil Mottola, and Dean L. Preston

May 16, 2018

Los Alamos National Laboratory
Los Alamos, NM, 87545, USA

E-mail: dblaschke@lanl.gov, emil@lanl.gov, dean@lanl.gov

Abstract

The phonon wind mechanism, that is, the anharmonic interaction and scattering of phonons by a moving dislocation, imparts a drag force $B(v,T,\rho)\,v$ on the dislocation. The drag coefficient B has been previously computed and experimentally determined only for dislocation velocities v much less than transverse sound speed, c_{T}. In this paper we derive an expression for the velocity dependence of B up to c_{T} in terms of the third-order elastic constants of the crystal. We compute the velocity dependence of the phonon wind contribution to B in the range 1%–90% c_{T} for Al, Cu, Fe, and Nb in the isotropic Debye approximation, and to better accuracy than in earlier studies. It is proved that the drag coefficient for screw dislocations scattering transverse phonons is finite as $v \to c_{\mathrm{T}}$, whereas B is divergent for edge dislocations scattering transverse phonons in the same limit. We compare our results to experimental results wherever possible and identify ways to validate and further improve the theory with more realistic phonon dispersion relations, MD simulations, and more accurate measurements.

Contents

1 Introduction and Outline

Dislocations are curvilinear defects in the crystal structure of the metal. The dislocations move, or glide through the crystal in an applied stress field at a speed that is controlled by two mechanisms. At low to intermediate plastic strain rates ($\leq 10^5 \mathrm{s}^{-1}$) the speed of the mobile dislocations is limited by their interactions with immobile (forest) dislocations that result in the formation of dislocation-dislocation nodes and short junctions. At finite temperature, the combination of the applied stress and local stress fluctuations arising from atomic oscillations result in dissociation of the nodes, hence continued glide. The rate-controlling intersection of non-coplanar, attractive mobile and immobile dislocations has traditionally been described by Van't Hoff-Arrhenius thermal activation theory, but this approach breaks down at high strain rates, so it was recently generalized to strain rates of nearly $10^{12}\mathrm{s}^{-1}$ [1]. At high strain rates ($\geq 10^5 \mathrm{s}^{-1}$) the dislocation speed is limited by both dislocation-dislocation interactions and viscous drag; the drag increases with the strain rate ($\sim$ dislocation speed). The drag force per unit length of dislocation is $B(v, T, \rho)\, v$ where B is the dislocation drag coefficient, v is the dislocation velocity, T is the temperature, and ρ is the material density. The drag coefficient is essential for models of single-crystal plasticity, polycrystal plasticity, and ductile failure applicable at high stresses and strain rates. In this high stress regime, where mean dislocation speeds vary from a few percent of transverse sound speed, c_{T}, up to nearly c_{T}, the dominant contribution to the dislocation drag coefficient is the scattering of phonons by the moving dislocations; in the rest frame of a moving dislocation the phonons moving past the dislocation act as a 'phonon wind' opposing its

glide through the crystal. Other dissipative effects, which we do not touch upon in this paper as they are subleading in the regimes of interest, are the thermoelastic damping and the radiation damping mechanisms, discussed for example in Ref. [2].

At low velocities, *i.e.* velocities less than a few percent of transverse sound speed, the drag coefficient due to phonon wind is roughly constant, but at higher velocities the drag coefficient increases nonlinearly. We note that existing continuum scale models of dislocation drag assume that the dislocation velocity is much smaller than c_{T}. There is currently no theoretical framework available in the literature for the accurate calculation of the velocity dependence of the dislocation drag coefficient up to c_{T}. Accordingly, the main focus of this paper is the development of such a framework: earlier first-principles continuum models of dislocation drag due to phonon wind are extended from low velocities to nearly c_{T}. The same framework also provides the temperature dependence of the drag coefficient up to velocities in the neighborhood of c_{T}, and is flexible enough to incorporate more realistic dispersion curves (the Debye approximation is used here) as well as more accurate experimental or numerical (quantum molecular dynamics) data on third-order elastic constants.

In this paper we restrict our study to velocities comparable to but strictly less than c_{T}, and dislocation-dislocation interactions are neglected. The case of supersonic dislocations is interesting in its own right, not least because of recent MD simulations and experiments that indicate the existence of dislocations moving at supersonic speeds in certain specialized materials such as liquid crystals or plasma crystals; see [3–6] and references therein. The extension of the theory to include dislocations moving at supersonic speeds, and dislocation-dislocation interactions, will be left for future work.

The outline of the paper is as follows. In order to provide a self-contained presentation, in Section 2 we expand the crystal potential in terms of displacements from the perfect lattice [7] to obtain the crystal Hamiltonian. We then consider a number of approximations and simplifications, such as the restriction to monatomic lattices, and the assumption of material isotropy. We employ the Debye approximation for the phonon spectrum. These simplifying approximations enable a semi-analytic approach in which experimentally determined second- and third-order elastic constants are used rather than numerical data from classical or quantum MD simulations. In Section 3 we discuss the displacement fields of edge and screw dislocations following Eshelby [8] and [9], and references therein. Section 4 is devoted to the phonon wind contribution to the drag coefficient in the continuum approximation. With the Debye approximation for the phonon spectrum, most of the computation of the drag coefficient can be performed analytically, leaving only a three-dimensional integral that is evaluated numerically. In Section 5 we present and discuss our results for a number of metals and compare to experimental values and MD simulations.

2 Isotropic Solids: Hamiltonian and Elastic Constants

In this section we provide a short review of the elements of continuum elasticity theory pertinent to the calculation of the drag coefficient.

2.1 Hamiltonian for an Isotropic Crystal

The Hamiltonian of a crystalline lattice can be expressed in the form

$$H = \frac{1}{2}\sum_{A} M^{(A)}\dot{\mathbf{r}}^{(A)\,2} + \Phi\{\mathbf{r}^{(A)}\} \tag{2.1}$$

where $M^{(A)}$ is the mass of the atom at lattice site A, $\{\mathbf{r}^{(A)}\}$ is the set of all atomic position vectors, and $\Phi\{\mathbf{r}^{(A)}\}$ is the crystal potential energy function. The crystal potential Φ may be expanded in a Taylor series about the set of equilibrium lattice positions $\{\mathbf{R}^{(A)}\}$,

$$\Phi\{\mathbf{r}\} = \Phi\{\mathbf{R}\} + \sum_{A,i} \Phi_i^{(A)} u_i^{(A)} + \frac{1}{2} \sum_{AB,ij} \Phi_{ij}^{(AB)} u_i^{(A)} u_j^{(B)} + \frac{1}{3!} \sum_{ABC,ijk} \Phi_{ijk}^{(ABC)} u_i^{(A)} u_j^{(B)} u_k^{(C)} + \dots \quad (2.2)$$

where

$$u_i^{(A)} \equiv r_i^{(A)} - R_i^{(A)} \quad (2.3)$$

are the Cartesian components $i = x, y, z$ of the displacement of atom A from its equilibrium position $\mathbf{R}^{(A)}$, $\{\mathbf{r}\} \equiv \{\mathbf{r}^{(A)}\}$, $\{\mathbf{R}\} \equiv \{\mathbf{R}^{(A)}\}$, and

$$\Phi_i^{(A)} = \left. \frac{\partial \Phi}{\partial r_i^{(A)}} \right|_{\{\mathbf{r}\}=\{\mathbf{R}\}} = 0 \,, \quad (2.4a)$$

$$\Phi_{ij}^{(AB)} = \left. \frac{\partial^2 \Phi}{\partial r_i^{(A)} \partial r_j^{(B)}} \right|_{\{\mathbf{r}\}=\{\mathbf{R}\}} , \quad (2.4b)$$

$$\Phi_{ijk}^{(ABC)} = \left. \frac{\partial^3 \Phi}{\partial r_i^{(A)} \partial r_j^{(B)} \partial r_k^{(C)}} \right|_{\{\mathbf{r}\}=\{\mathbf{R}\}} . \quad (2.4c)$$

Since the $\{\mathbf{R}^{(A)}\}$ are the equilibrium positions of the atoms, the first variation of $\Phi\{\mathbf{r}\}$ with respect to the $u_i^{(A)}$, (2.4a), vanishes.

In the continuum limit the displacement field is a continuous function of position, $u_i^{(A)} \equiv u_i(\mathbf{R}^{(A)}) \to u_i(\mathbf{x})$, and we have the nine displacement gradients

$$u_{i,j} \equiv \frac{\partial u_i}{\partial x_j} \,. \quad (2.5)$$

We now consider a homogeneous deformation of the lattice, that is, a deformation for which the gradients are constants

$$u_i^{(A)} = u_{i,j} \, R_j^{(A)} \,. \quad (2.6)$$

Substituting this into (2.2) we obtain

$$\Phi\{\mathbf{r}\} = \Phi\{\mathbf{R}\} + \frac{V}{2} \sum_{ijkl} C_{ij}^{kl} \, u_{i,k} \, u_{j,l} + \frac{V}{6} \sum_{ijklmn} D_{ijk}^{lmn} \, u_{i,l} \, u_{j,m} \, u_{k,n} + \dots \quad (2.7)$$

where the elastic constants are defined by

$$C_{ij}^{kl} \equiv \frac{1}{V} \sum_{AB} \Phi_{ij}^{(AB)} R_k^{(A)} R_l^{(B)} \,, \quad (2.8a)$$

$$D_{ijk}^{lmn} \equiv \frac{1}{V} \sum_{ABC} \Phi_{ijk}^{(ABC)} R_l^{(A)} R_m^{(B)} R_n^{(C)} \,. \quad (2.8b)$$

Since summing over all lattice sites in (2.8) results in an extensive quantity, proportional to the total number of lattice sites and hence to the total volume of the crystal, the factor of the total volume V is extracted explicitly from definitions of the elastic constants (2.8) to yield intensive quantities independent of the total volume.

Assuming that the displacements are slowly varying over the lattice, hence the dimensionless gradients are small and slowly varying, the continuum Hamiltonian follows from (2.7)

$$H = \int d^3\mathbf{x} \left\{ \frac{1}{2}\,\rho_0 \sum_i \dot{u}_i^2 + \frac{1}{2} \sum_{ijkl} C_{ij}^{kl}\, u_{i,k}\, u_{j,l} + \frac{1}{6} \sum_{ijklmn} D_{ijk}^{lmn}\, u_{i,l}\, u_{j,m}\, u_{k,n} \right\} + \dots \quad . \tag{2.9}$$

Variation of the Hamiltonian yields the equation of motion for the continuous displacement field

$$\rho_0 \frac{\partial^2 u_i}{\partial t^2} = \sum_{jkl} C_{ij}^{kl} \frac{\partial^2 u_j}{\partial x_k \partial x_l} + \sum_{jklmn} D_{ijk}^{lmn} \frac{\partial}{\partial x_l} \left(\frac{\partial u_j}{\partial x_m} \frac{\partial u_k}{\partial x_n} \right) + \dots \tag{2.10}$$

where

$$\rho_0 = \frac{1}{V} \sum_A M^{(A)} \tag{2.11}$$

is the average equilibrium mass density. The harmonic approximation of linear elastic displacements is obtained by neglect of all terms beyond the linear ones in (2.10), and treating the next order anharmonic terms involving D_{ijk}^{lmn} as a small perturbation to the linear approximation. We emphasize that this linear and weak anharmonic approximation is restricted to the limit where the dimensionless gradients (2.5) are both small compared to unity *and* slowly varying on the distance scale of the underlying crystal lattice.

The variation of the integrand of the potential term in the Hamiltonian (2.9), *i.e.*

$$\sum_{ij} \tau_{ij}\, du_{i,j} = \sum_{ijkl} C_{ij}^{kl}\, u_{j,l}\, du_{i,k} + \frac{1}{2} \sum_{ijklmn} D_{ijk}^{lmn}\, u_{j,m}\, u_{k,n}\, du_{i,l} + \dots \tag{2.12}$$

provides the stress tensor

$$\tau_{ij} = \sum_{kl} C_{ik}^{jl}\, u_{k,l} + \frac{1}{2} \sum_{ijklmn} D_{ikl}^{jmn}\, u_{k,m}\, u_{l,n} + \dots \tag{2.13}$$

in terms of the displacement gradients. It follows from angular momentum conservation that the stress tensor is symmetric, hence it depends only on the symmetric part of $u_{i,j}$, that is, the infinitesimal strain

$$u_{(i,j)} = \frac{1}{2}(u_{i,j} + u_{j,i}) \equiv \epsilon_{ij}\,. \tag{2.14}$$

The antisymmetric part of the displacement gradient

$$u_{[i,j]} = \frac{1}{2}(u_{i,j} - u_{j,i}) \equiv \omega_{ij}\,. \tag{2.15}$$

is pure rotation. Both small deformations of the crystal lattice, as well as the relatively larger dislocations, generally contain regions with both symmetric and antisymmetric gradients.

2.2 Second-order Elastic Constants and Phonons

Although bulk continuum quantities, the form of the elastic tensors C_{ij}^{kl} and D_{ijk}^{lmn} still depend upon the underlying discrete symmetry group of the crystal. However, for polycrystals a reasonable approximation is obtained by averaging over directions and assuming that the undeformed crystal can be treated as homogeneous and isotropic. In that case the number of independent tensors that can appear in C_{ij}^{kl} and D_{ijk}^{lmn} is greatly reduced. The integrand in the Hamiltonian

(2.9) must be a rotationally invariant scalar, and there are only two such independent scalars at second order in $\mathbf{u}$, namely

$$(\nabla \cdot \mathbf{u})^2 = \big(u_{i,i}\big)^2 \qquad \text{and} \qquad (\nabla \times \mathbf{u})^2 = 2\,\omega_{ij}\,\omega_{ij} = u_{i,j}^2 - u_{i,j}u_{j,i} \tag{2.16}$$

involving only the symmetric and anti-symmetric parts of the displacement gradient respectively. The continuum isotropic potential may be expressed in the form

$$\mathcal{U}_2 = \frac{1}{2}\,(\lambda + 2\mu) \int d^3\mathbf{x}\,(\nabla \cdot \mathbf{u})^2 + \frac{1}{2}\,\mu \int d^3\mathbf{x}\,(\nabla \times \mathbf{u})^2 \tag{2.17}$$

at second order in the displacement gradients $u_{i,j}$, where λ and μ are the (positive) Lamé coefficients. Up to an integration by parts and surface contribution this corresponds to

$$C_{ij}^{kl} = \lambda\,\delta_{ik}\delta_{jl} + \mu\,(\delta_{ij}\delta_{kl} + \delta_{il}\delta_{jk}) \tag{2.18}$$

and leads to the linearized continuum eqs. of motion [10, 11]

$$\rho_0\,\frac{\partial^2 \mathbf{u}}{\partial t^2} = \mu\,\nabla^2\mathbf{u} + (\lambda + \mu)\,\nabla(\nabla \cdot \mathbf{u}\,) \tag{2.19}$$

for the displacement vector field $\mathbf{u}(\mathbf{x}, t)$, in which the anharmonic terms have been neglected. The Lamé constants μ, λ are related to the bulk and shear moduli B and G via $G = \mu - P$ and $B + \frac{4}{3}G = \lambda + 2\mu - P$. Here, however, we neglect pressure and hence assume $P \approx 0$.

Since any vector $\mathbf{u}$ can be separated into its transverse (T) and longitudinal (L) parts by

$$u_i = u_i^{(\mathrm{T})} + u_i^{(\mathrm{L})} = \left(u_i - \partial_i \frac{1}{\nabla^2}\partial_j u_j\right) + \partial_i \frac{1}{\nabla^2}\partial_j u_j \tag{2.20}$$

with $\nabla \cdot \mathbf{u}^{(\mathrm{T})} = 0$, which are orthogonal, the linearized continuum eq. (2.19) separates into two independent linear equations

$$\rho_0\,\frac{\partial^2 \mathbf{u}^{(\mathrm{T})}}{\partial t^2} = \mu\,\nabla^2\mathbf{u}^{(\mathrm{T})} \tag{2.21a}$$

$$\rho_0\,\frac{\partial^2 \mathbf{u}^{(\mathrm{L})}}{\partial t^2} = (\lambda + 2\mu)\,\nabla(\nabla \cdot \mathbf{u}^{(\mathrm{L})}\,) \tag{2.21b}$$

for the transverse and longitudinal displacements respectively. Each of these equations has the form of a wave equation, but with a different speed of propagation, depending upon whether the particle motion is transverse or longitudinal (*i.e.* parallel) to its direction of propagation.

The transverse and longitudinal sound wave solutions of (2.19) are easily found. The two transverse modes are

$$u_i^{(\mathrm{T})}(\mathbf{x}, t|\mathbf{k}, s) = \mathrm{e}_i(\mathbf{k}, s)\,e^{i\mathbf{k}\cdot\mathbf{x} - i\omega_{\mathrm{T}}t}\,, \qquad\qquad \mathbf{k} \cdot \mathbf{e}(\mathbf{k}, s) = 0 \tag{2.22}$$

with dispersion relation and sound speed

$$\omega_{\mathrm{T}}(k) = c_{\mathrm{T}}k\,, \qquad\qquad c_{\mathrm{T}} = \sqrt{\frac{\mu}{\rho_0}}\,, \tag{2.23}$$

where $k \equiv |\mathbf{k}|$ and $s = 1, 2$ labels the two unit polarization vectors $\mathbf{e}_{Ts}$ transverse to the direction of propagation $\hat{\mathbf{k}}$. The longitudinal mode

$$u_i^{(\mathrm{L})}(\mathbf{x}, t|\mathbf{k}) = \mathrm{e}_i(\mathbf{k}, 3)\,e^{i\mathbf{k}\cdot\mathbf{x} - i\omega_{\mathrm{L}}t}\,, \qquad\qquad \mathbf{k} \times \mathbf{e}(\mathbf{k}, 3) = 0 \tag{2.24}$$

with displacements in the direction of propagation, has dispersion relation and sound speed

$$\omega_{\rm L}(k) = c_{\rm L} k\,, \qquad\qquad c_{\rm L} = \sqrt{\frac{\lambda+2\mu}{\rho_0}} > c_{\rm T}\,. \tag{2.25}$$

To simplify the notation the polarization indices $s, s' = 1, 2$ label the two transverse sound modes, and $s = 3$ or $s' = 3$ labels the single longitudinal mode, so that the polarization vectors satisfy

$$\sum_{i=1,2,3} {\rm e}_i(\mathbf{k}, s)\, {\rm e}_i(\mathbf{k}, s') = \delta_{ss'} \qquad \text{and} \qquad \sum_{s=1,2,3} {\rm e}_i(\mathbf{k}, s)\, {\rm e}_j(\mathbf{k}, s) = \delta_{ij} \tag{2.26}$$

and form an orthonormal basis set. Additionally, they satisfy (2.26) and ${\rm e}_i(-\mathbf{k}, s) = {\rm e}_i^*(\mathbf{k}, s)$. Note that because the transverse modes have non-zero curl, and $(\nabla \times \mathbf{u})_i = \varepsilon_{ijk}\omega_{jk}$ they provide a non-vanishing antisymmetric gradient field $\omega_{ij} \neq 0$.

The small elastic displacement fields may be quantized in terms of three phonon modes by

$$u_i(\mathbf{x}, t)\Big|_{\rm phonon} = \sqrt{\frac{\hbar}{\rho_0}} \sum_s \int \frac{d^3\mathbf{k}}{(2\pi)^3} \frac{1}{\sqrt{2\omega_s(k)}} \left\{ \hat{a}_s(\mathbf{k}) e^{i\mathbf{k}\cdot\mathbf{x} - i\omega_s t} + \hat{a}_s^\dagger(\mathbf{k}) e^{-i\mathbf{k}\cdot\mathbf{x} + i\omega_s t} \right\} {\rm e}_i(\mathbf{k}, s) \tag{2.27}$$

where the phonon creation and destruction operators are quantized with the continuum normalization

$$[\hat{a}_s(\mathbf{k}), \hat{a}_{s'}^\dagger(\mathbf{k}')] = (2\pi)^3\, \delta^3(\mathbf{k} - \mathbf{k}')\, \delta_{ss'} \tag{2.28}$$

in the infinite volume limit. Note also that at the linear order of continuum elastic theory the phonon modes necessarily have gapless linear dispersion relations $\omega_{\rm T}(\mathbf{k}) = c_{\rm T} k$, $\omega_{\rm L}(\mathbf{k}) = c_{\rm L} k$, characteristic of the Debye approximation.

2.3 Third-order Elastic Constants for an Isotropic Solid

For the third order potential energy involving the elastic constants D_{ijk}^{lmn} there exist five distinct independent scalars involving three displacement gradients, and the third order potential in (2.9) is

$$\begin{aligned}
\mathcal{U}_3 =& \int d^3\mathbf{x} \left\{ a\,(\epsilon_{ii})^3 + b\,\epsilon_{ii}\epsilon_{jk}\epsilon_{jk} + c\,\epsilon_{ij}\epsilon_{jk}\epsilon_{ki} + g\,\epsilon_{ii}(\varepsilon_{njk}\omega_{jk})(\varepsilon_{nlm}\omega_{lm}) + h\,\epsilon_{ij}(\varepsilon_{ikl}\omega_{kl})(\varepsilon_{jmn}\omega_{mn}) \right\} \\
=& \int d^3\mathbf{x} \left\{ a\,(u_{i,i})^3 + \left(\frac{b}{2} + g + h\right) u_{i,i}\, u_{j,k}\, u_{j,k} + \left(\frac{b}{2} - g - h\right) u_{i,i}\, u_{j,k}\, u_{k,j} \right. \\
& \left. + \left(\frac{c}{4} + h\right) u_{i,j}\, u_{j,k}\, u_{k,i} + \left(\frac{3c}{4} - h\right) u_{i,j}\, u_{i,k}\, u_{k,j} \right\}
\end{aligned} \tag{2.29}$$

where the a, b, c coefficients multiply terms which are totally symmetric (denoted SSS) while the g, h coefficients multiply terms with one symmetric, two antisymmetric gradients (denoted SAA). Terms with odd powers of the antisymmetric gradients (SSA or AAA) are odd under parity and do not appear in $\mathcal{U}_3$ if we assume that the isotropic crystal is symmetric with respect to reflections about any plane.

The five coefficients of the third-order terms in (2.29) are in general independent of each other and the second-order Lamé constants λ and μ, and in general all five coefficients can be non-zero and should be allowed. It appears however that the independence of the third-order SAA elastic constants g, h from the a, b, c and λ, μ elastic constants has not been fully taken into account in the previous literature. This is due to the fact that only the symmetrized strain field

ϵ_{ij} has been considered relevant, and the independent SAA g, h terms in the third-order elastic energy have been neglected. Instead an expansion in the non-linear strain field (also known Murnaghan strain [12] or Green-Saint-Venant strain tensor [13])

$$\eta_{ij} = \epsilon_{ij} + \frac{1}{2}\frac{\partial u_k}{\partial x_i}\frac{\partial u_k}{\partial x_j}\,, \tag{2.30}$$

which is fully symmetric in indices i, j has been employed. Then if the two independent SAA constants are set to zero in $\mathcal{U}_3$, but the total potential

$$\frac{1}{2}C_{ij}^{kl}\eta_{ik}\eta_{jl} + \frac{1}{6}\tilde{D}_{ijk}^{lmn}\eta_{il}\eta_{jm}\eta_{kn}$$

with [1]

$$\begin{aligned}\tilde{D}_{ijk}^{lmn} \equiv D_{ijk}^{lmn}(a,b,c\to\tilde{a},\tilde{b},\tilde{c})\Big|_{g=h=0} &= 6\,\tilde{a}\,\delta_{il}\delta_{jm}\delta_{kn}\\ &+ \tilde{b}\left[\delta_{il}\left(\delta_{jk}\delta_{mn}+\delta_{jn}\delta_{mk}\right)+\delta_{jm}\left(\delta_{ik}\delta_{ln}+\delta_{in}\delta_{lk}\right)+\delta_{kn}\left(\delta_{ij}\delta_{lm}+\delta_{im}\delta_{lj}\right)\right]\\ &+ \frac{3\,\tilde{c}}{4}\left[\delta_{ij}\left(\delta_{lk}\delta_{mn}+\delta_{ln}\delta_{mk}\right)+\delta_{lm}\left(\delta_{ik}\delta_{jn}+\delta_{in}\delta_{jk}\right)\right.\\ &\qquad\left.+\delta_{im}\left(\delta_{lk}\delta_{jn}+\delta_{ln}\delta_{jk}\right)+\delta_{lj}\left(\delta_{ik}\delta_{mn}+\delta_{in}\delta_{mk}\right)\right]\end{aligned} \tag{2.31}$$

is expanded up to third order in the gradients $u_{i,j}$, one obtains an *effective* third-order elastic tensor [7, 16]

$$D_{ijk}^{lmn} = \tilde{D}_{ijk}^{lmn} + C_{im}^{ln}\delta_{jk} + C_{jl}^{mn}\delta_{ik} + C_{lk}^{mn}\delta_{ij}\,, \tag{2.32}$$

containing an admixture of the second-order λ, μ coefficients. Indeed in this way one obtains the same polynomial for $\mathcal{U}_3$ as (2.29), but with

$$a = \tilde{a}\,, \qquad b = \tilde{b} + \frac{1}{2}\,\lambda\,, \qquad c = \tilde{c} + \mu\,, \tag{2.33a}$$

$$g = \frac{1}{4}\,(\lambda+\mu)\,, \qquad h = -\frac{1}{4}\,\mu\,, \tag{2.33b}$$

with the SAA terms effectively generated only by the lower-order Lamé coefficients λ, μ, instead of being truly independent third-order constants as they should be. Since $\mathcal{U}_3$ was expanded in terms of η_{ij} rather than the general displacement gradients $u_{i,j} = \epsilon_{ij} + \omega_{ij}$ containing both symmetric and antisymmetric terms, no independent third-order constants appear within g and h (which is consistent with the earlier literature as pointed out above). It is clear even at linearized order of phonon excitations that the antisymmetric gradients ω_{ij} are present since $\mathrm{e}_i(\mathbf{k}, s)k_j \neq \mathrm{e}_j(\mathbf{k}, s)k_i$ for the transverse polarizations $s = 1, 2$.

Finally, the third-order elastic constants $\tilde{a}$, $\tilde{b}$, and $\tilde{c}$ are related to the well-known Murnaghan constants, $\mathfrak{l}$, $\mathfrak{m}$, $\mathfrak{n}$, as follows:

$$\tilde{a} = \frac{1}{3}\,(\mathfrak{l}-\mathfrak{m}) + \frac{1}{6}\mathfrak{n}\,, \qquad \tilde{b} = \mathfrak{m} - \frac{1}{2}\mathfrak{n}\,, \qquad \tilde{c} = \frac{1}{3}\mathfrak{n}\,. \tag{2.34}$$

[1] Ref. [14] writes the same general expression for the isotropic third-order elastic constants using $\nu_1 = 6\tilde{a}$, $\nu_2 = \tilde{b}$, and $\nu_3 = 3\tilde{c}/4$. According to Ref. [15], the ν_i are related to the Murnaghan constants via $\mathfrak{l} = \nu_2 + \nu_1/2$, $\mathfrak{m} = 2\nu_3 + \nu_2$, and $\mathfrak{n} = 4\nu_3$. Presently, this leads us to eq. (2.34).

The metals we are interested in have cubic I symmetry and are therefore described by three second-order and six third-order elastic constants. However, if we consider polycrystals, isotropy is a reasonable assumption, and the effective isotropic constants are averaged quantities. Because of high uncertainties in the theoretical averaging procedure when effective isotropic constants are computed from the single-crystal cubic ones [17, 18], we have refrained here from doing so. Instead, we have used experimentally measured effective isotropic constants; see Table 1 in Section 5.

3 Edge and Screw Dislocations: Displacement Fields

An infinite edge dislocation along the $\hat{\mathbf{z}}$ axis with Burgers vector in the $\hat{\mathbf{x}}$ direction is described by the displacement vector $\mathbf{d}(\mathbf{x})$ with components [19, 20]

$$d_x(x,y) = \frac{b}{2\pi}\left\{\tan^{-1}\left(\frac{y}{x}\right) + \left(\frac{\lambda+\mu}{\lambda+2\mu}\right)\frac{xy}{x^2+y^2}\right\} \tag{3.1a}$$

$$d_y(x,y) = \frac{b}{2\pi}\left(\frac{1}{\lambda+2\mu}\right)\left\{-\frac{\mu}{2}\ln\left(\frac{x^2+y^2}{r_0^2}\right) + (\lambda+\mu)\frac{y^2}{x^2+y^2}\right\} \tag{3.1b}$$

$$d_z = 0 \tag{3.1c}$$

where b is the magnitude of the Burgers' vector, and r_0 is the dislocation core radius. Similarly an infinite screw dislocation along the $\hat{\mathbf{z}}$ axis is described by the displacement vector $\mathbf{d}(\mathbf{x})$ with components [19, 20]

$$d_x = d_y = 0 \tag{3.2a}$$

$$d_z(x,y) = \frac{b}{2\pi}\tan^{-1}\left(\frac{y}{x}\right) \tag{3.2b}$$

whose Burgers vector $\mathbf{b} = b\hat{\mathbf{z}}$ in the $\hat{\mathbf{z}}$ direction. Each of these dislocation displacements are solutions of the equations of linearized static continuum elasticity (2.19), everywhere except at the origin $x = y = 0$, where they are singular. The edge dislocation (3.1) contains both longitudinal (L) components with zero curl and transverse components (T) with zero divergence, whereas the screw dislocation (3.2) is purely transverse (T). The non-zero transverse displacements have anti-symmetric rotation strain fields, hence $\omega_{ij} = u_{[i,j]} \neq 0$, and both dislocations have non-zero internal torques.

In order to find the solutions of the linear elastic eqs. (2.19) for dislocations moving with uniform velocity $\mathbf{v} = v\hat{\mathbf{x}}$ (with $\hat{\boldsymbol{\xi}} = \hat{\mathbf{z}}$, $\hat{\mathbf{b}} = \hat{\mathbf{x}}$), Eshelby decomposed the stationary edge dislocation (3.1) into its transverse and longitudinal parts, using the effective Lorentz invariance of the eqs. (2.21), and obtained [8]

$$\begin{aligned}
d_x(x,y;t) &= \frac{b}{\pi\beta_{\mathrm{T}}^2}\left\{\tan^{-1}\left[\frac{y}{\gamma_{\mathrm{L}}(x-vt)}\right] - \left(1-\frac{\beta_{\mathrm{T}}^2}{2}\right)\tan^{-1}\left[\frac{y}{\gamma_{\mathrm{T}}(x-vt)}\right]\right\}, \\
d_y(x,y;t) &= \frac{b}{2\pi\beta_{\mathrm{T}}^2}\left\{\frac{1}{\gamma_{\mathrm{L}}}\ln\left[\frac{(x-vt)^2+y^2/\gamma_{\mathrm{L}}^2}{r_0^2}\right] - \gamma_{\mathrm{T}}\left(1-\frac{\beta_{\mathrm{T}}^2}{2}\right)\ln\left[\frac{(x-vt)^2+y^2/\gamma_{\mathrm{T}}^2}{r_0^2}\right]\right\},
\end{aligned} \tag{3.3}$$

for an edge dislocation gliding in an isotropic elastic solid in the x direction with uniform velocity v, where

$$\beta_{T,L} \equiv \frac{v}{c_{T,L}}, \qquad \gamma_{T,L} = \sqrt{\frac{1}{1-\beta_{T,L}^2}}, \tag{3.4}$$

following the standard notations of special relativity [2]. We consider below only gliding edge and screw dislocations, as dislocation climb is highly suppressed and hence can be neglected in the discussion of phonon wind [21].

One may check that $d_{x,y}$ above indeed satisfy eq. (2.19). In fact, one may check that the first (resp. second) terms of $\mathbf{d}(x,y;t)$ depending only on $\gamma_{\rm L}$ (resp. $\gamma_{\rm T}$) satisfy eq. (2.21) independently of each other. However, only with this particular combination in (3.3) will no external concentrated force need to be applied in the y-direction at the core of the dislocation (where $x=y=0$), see e.g. [9]. We note that d_y differs from some other results found in the literature by an arbitrary constant. For example, if we take the limit $v\to 0$ in (3.3) (and neglect the regulator, i.e. $r_0\to 1$) and express the results in terms of the Poisson ratio $\nu=\lambda/2(\mu+\lambda)$, our expression for d_y differs from those in Ref. [11] by a constant $b/8\pi(1-\nu)$, but agrees with the original result of Burgers [19]. Since the interaction Hamiltonian (4.6) depends only on the gradient of the dislocation displacement, this additive constant is of no physical relevance.

The gradients of the dislocation displacement field (3.3) are

$$
\begin{aligned}
&d_{i,j}:=\partial_j d_i\,,\\
&d_{x,x}=\frac{-by}{\pi\beta_{\rm T}^2}\left(\frac{1/\gamma_{\rm L}}{((x-tv)^2+y^2/\gamma_{\rm L}^2)}-\frac{\left(1-\frac{\beta_{\rm T}^2}{2}\right)/\gamma_{\rm T}}{((x-tv)^2+y^2/\gamma_{\rm T}^2)}\right),\\
&d_{x,y}=\frac{b(x-tv)}{\pi\beta_{\rm T}^2}\left(\frac{1/\gamma_{\rm L}}{((x-tv)^2+y^2/\gamma_{\rm L}^2)}-\frac{\left(1-\frac{\beta_{\rm T}^2}{2}\right)/\gamma_{\rm T}}{((x-tv)^2+y^2/\gamma_{\rm T}^2)}\right),\\
&d_{y,x}=\frac{b(x-tv)}{\pi\beta_{\rm T}^2}\left(\frac{1/\gamma_{\rm L}}{((x-tv)^2+y^2/\gamma_{\rm L}^2)}-\frac{\gamma_{\rm T}\left(1-\frac{\beta_{\rm T}^2}{2}\right)}{((x-tv)^2+y^2/\gamma_{\rm T}^2)}\right),\\
&d_{y,y}=\frac{by}{\pi\beta_{\rm T}^2}\left(\frac{1/\gamma_{\rm L}^3}{((x-tv)^2+y^2/\gamma_{\rm L}^2)}-\frac{\left(1-\frac{\beta_{\rm T}^2}{2}\right)/\gamma_{\rm T}}{((x-tv)^2+y^2/\gamma_{\rm T}^2)}\right),
\end{aligned}
\tag{3.5}
$$

or written in polar coordinates at time $t=0$:

$$
\begin{aligned}
d_{x,x}(r,\theta)&=\frac{-b\sin\theta}{\pi\beta_{\rm T}^2 r}\left(\frac{1/\gamma_{\rm L}}{(1-\beta_{\rm L}^2\sin^2\theta)}-\frac{\left(1-\frac{\beta_{\rm T}^2}{2}\right)/\gamma_{\rm T}}{(1-\beta_{\rm T}^2\sin^2\theta)}\right),\\
d_{x,y}(r,\theta)&=\frac{b\cos\theta}{\pi\beta_{\rm T}^2 r}\left(\frac{1/\gamma_{\rm L}}{(1-\beta_{\rm L}^2\sin^2\theta)}-\frac{\left(1-\frac{\beta_{\rm T}^2}{2}\right)/\gamma_{\rm T})}{(1-\beta_{\rm T}^2\sin^2\theta)}\right),\\
d_{y,x}(r,\theta)&=\frac{b\cos\theta}{\pi\beta_{\rm T}^2 r}\left(\frac{1/\gamma_{\rm L}}{(1-\beta_{\rm L}^2\sin^2\theta)}-\frac{\left(1-\frac{\beta_{\rm T}^2}{2}\right)\gamma_{\rm T}}{(1-\beta_{\rm T}^2\sin^2\theta)}\right),
\end{aligned}
$$

[2] Note that our definition of γ differs from Eshelby by $\gamma\to 1/\gamma$.

$$d_{y,y}(r,\theta) = \frac{b\sin\theta}{\pi\beta_{\rm T}^2 r}\left(\frac{1/\gamma_{\rm L}^3}{(1-\beta_{\rm L}^2\sin^2\theta)} - \frac{\left(1-\frac{\beta_{\rm T}^2}{2}\right)/\gamma_{\rm T}}{(1-\beta_{\rm T}^2\sin^2\theta)}\right). \tag{3.6}$$

Note that the infinitesimal symmetric strain $\epsilon_{xy} = (d_{x,y} + d_{y,x})/2$ vanishes at $y = 0$ (resp. $\sin\theta = 0$) at a dislocation velocity $v = c_{\rm R}$ which satisfies the relation $\gamma_{\rm L}\gamma_{\rm T} = (1-\beta_{\rm T}^2/2)^{-2}$. This velocity is known as the Rayleigh wave velocity (which is the velocity of surface waves) [9, 20], and is always smaller than (but fairly close to) the transverse sound speed, $c_{\rm R} < c_{\rm T}$, a typical value being $c_{\rm R} \approx 0.93 c_{\rm T}$.

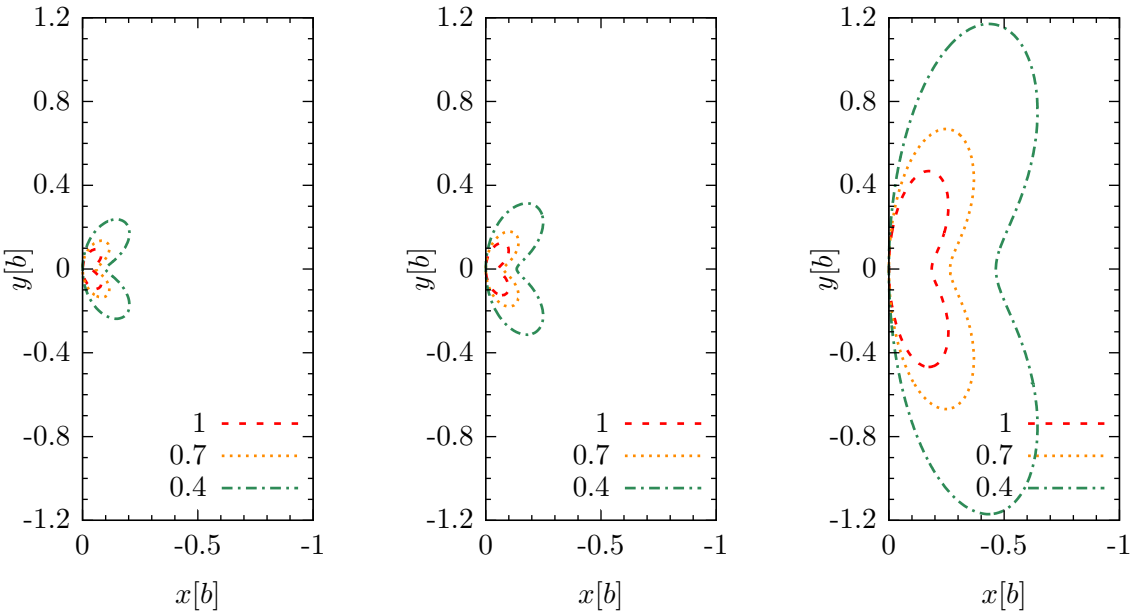

Figure 1: A component of the gradient of the displacement field of a edge dislocation, d_{yx} (assuming $c_{\rm L} \approx 2c_{\rm T}$), is shown (from left to right) for velocities $v = 0$, $v = 0.5c_t$, and $v = 0.9c_{\rm T}$. The latter leads to an enhanced gradient. An increase in the dislocation velocity is accompanied by expansion of the core region where linear elasticity, $d_{i,j} \ll 1$, breaks down. This expansion is more prominent perpendicular to v, i.e. in the y-direction.

The time-dependent displacement field of a screw dislocation with sense vector $\hat{\xi}$ along the positive z-axis, gliding in the x direction at velocity v, is given by [8]

$$d_z(x,y;t) = \frac{b}{2\pi}\tan^{-1}\left[\frac{y}{\gamma_{\rm T}(x-vt)}\right]. \tag{3.7}$$

One may check that d_z above indeed satisfies eq. (2.19). Its gradient is easily computed resulting in

$$d_{z,x} = -\frac{b\,y/\gamma_{\rm T}}{2\pi\left((x-tv)^2 + y^2/\gamma_{\rm T}^2\right)}, \qquad d_{z,y} = \frac{b\,(x-tv)/\gamma_{\rm T}}{2\pi\left((x-tv)^2 + y^2/\gamma_{\rm T}^2\right)}. \tag{3.8}$$

We now calculate the Fourier transforms of the moving edge and screw dislocation deformation fields for $\hat{\xi} = \hat{\mathbf{z}}$.

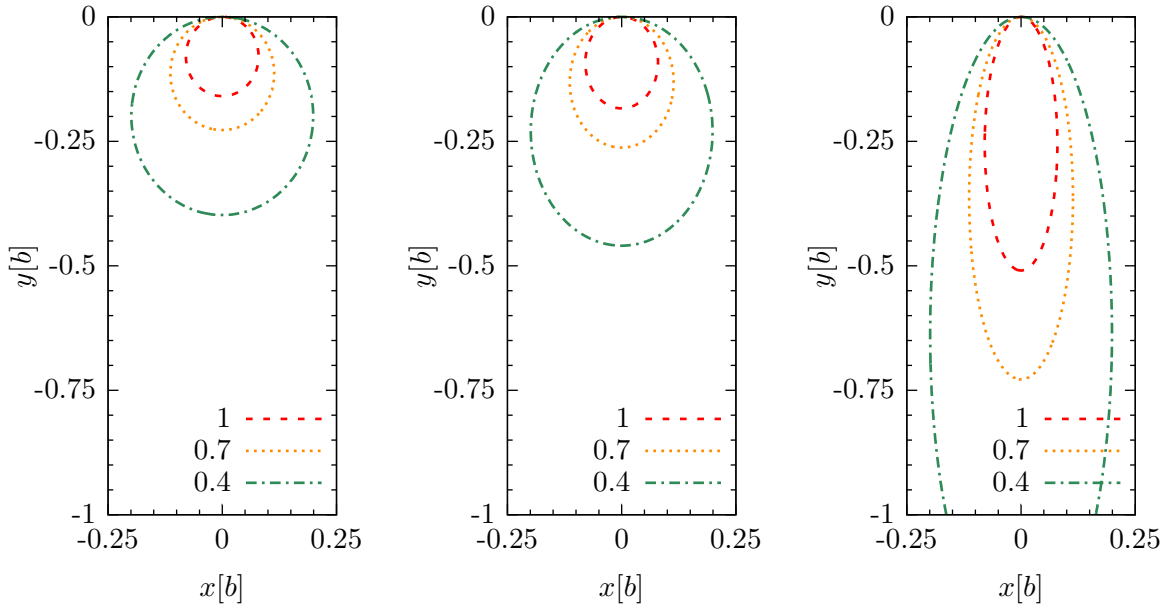

Figure 2: A component of the gradient of the displacement field of a screw dislocation, $d_{z,x}$, is shown (from left to right) for velocities $v = 0$, $v = 0.5c_t$, and $v = 0.95c_{\mathrm{T}}$. The latter leads to an enhanced gradient. An increase in the dislocation velocity is accompanied by expansion perpendicular to v (i.e. in the y-direction) of the core region where linear elasticity, $d_{i,j} \ll 1$, breaks down.

Neglecting the finite core size of the dislocation ($r_0 \to 0$), we define

$$\tilde{d}_{i,j}(q,\phi) = \int_0^\infty dr r \int_0^{2\pi} d\theta \, d_{i,j}(r,\theta) e^{-iqr\cos(\theta-\phi)} \,, \tag{3.9}$$

and get

$$\begin{aligned}
\tilde{d}_{x,x}(q,\phi) &= \frac{2ib\sin\phi}{\beta_{\mathrm{T}}^2 q}\left(\frac{1}{(1-\beta_{\mathrm{L}}^2\cos^2\phi)} - \frac{\left(1-\frac{\beta_{\mathrm{T}}^2}{2}\right)}{(1-\beta_{\mathrm{T}}^2\cos^2\phi)}\right), \\
\tilde{d}_{x,y}(q,\phi) &= \frac{-2ib\cos\phi}{\beta_{\mathrm{T}}^2 q}\left(\frac{\gamma_{\mathrm{L}}^{-2}}{(1-\beta_{\mathrm{L}}^2\cos^2\phi)} - \frac{\left(1-\frac{\beta_{\mathrm{T}}^2}{2}\right)\gamma_{\mathrm{T}}^{-2}}{(1-\beta_{\mathrm{T}}^2\cos^2\phi)}\right), \\
\tilde{d}_{y,x}(q,\phi) &= \frac{-2ib\cos\phi}{\beta_{\mathrm{T}}^2 q}\left(\frac{\gamma_{\mathrm{L}}^{-2}}{(1-\beta_{\mathrm{L}}^2\cos^2\phi)} - \frac{\left(1-\frac{\beta_{\mathrm{T}}^2}{2}\right)}{(1-\beta_{\mathrm{T}}^2\cos^2\phi)}\right), \\
\tilde{d}_{y,y}(q,\phi) &= \frac{-2ib\sin\phi}{\beta_{\mathrm{T}}^2 q}\left(\frac{\gamma_{\mathrm{L}}^{-2}}{(1-\beta_{\mathrm{L}}^2\cos^2\phi)} - \frac{\left(1-\frac{\beta_{\mathrm{T}}^2}{2}\right)}{(1-\beta_{\mathrm{T}}^2\cos^2\phi)}\right).
\end{aligned} \tag{3.10}$$

The details of the derivation leading to (3.10) as well as a short discussion on cutoffs taking into account the finite dislocation core size r_0 and the mean separation α of dislocations can be found in Appendix A. There we argue that neglecting both cutoffs will change our results by 10% or less, provided $r_0 < b/3$ and $\alpha > 50b$. The advantage of taking the limits $r_0 \to 0$ and $\alpha \to \infty$, on the other hand, is reflected in the simple expression (3.10) above.

The limitations of this approximation are illustrated in Figures 1 and 2. Although our estimate on the effect of the cutoffs should be adequate for a wide range of dislocation velocities, we expect a breakdown of the present theory close to transverse sound speed. The reason is that a core region where the assumption of small strains allowing the use of linear elasticity is invalid, becomes larger with increasing velocity. Therefore, we will limit our discussion in Section 5 to velocities $v \lesssim 0.9 c_{\mathrm{T}}$.

For later reference, we note that the trace of the edge dislocation's displacement gradient field simplifies to

$$\tilde{d}_{i,i}(q,\phi) = \tilde{d}_{x,x}(q,\phi) + \tilde{d}_{y,y}(q,\phi) = \frac{2ib\, c_{\mathrm{T}}^2 \sin\phi}{q\, c_{\mathrm{L}}^2 \left(1 - \beta_{\mathrm{L}}^2 \cos^2\phi\right)} \,. \tag{3.11}$$

Following the same steps as for edge dislocations, we find the Fourier transform of the corresponding displacement gradient field (without cutoffs) for the screw case:

$$\tilde{d}_{z,x}(q,\phi) = \frac{ib \sin\phi}{q\left(1 - \beta_{\mathrm{T}}^2 \cos^2\phi\right)} \,, \qquad \tilde{d}_{z,y}(q,\phi) = -\frac{ib\, \gamma_{\mathrm{T}}^{-2} \cos\phi}{q\left(1 - \beta_{\mathrm{T}}^2 \cos^2\phi\right)} \,; \tag{3.12}$$

all other components vanish.

4 The Phonon Wind Contribution to the Drag Coefficient

4.1 General Considerations

The thermal phonons in a crystal are scattered by gliding dislocations, thereby resulting in a drag force on the dislocations. By analogy with linear (Stokes) drag on objects moving through fluids at low velocities (low Reynolds numbers), the dislocation drag force per unit length is written

$$F = B\, v \,, \tag{4.1}$$

where $B = B(v,T)$ is the dislocation drag coefficient. At low velocities B is approximately independent of the dislocation velocity (see results below), hence the drag is approximately linear. Typical low-velocity values of B are in the range 10^{-4} – 10^{-3} Poise (10^{-2} – 10^{-1} mPa s). The energy dissipated per unit time per unit length of a dislocation is

$$D = F\, v = B\, v^2 \,. \tag{4.2}$$

In discussing dislocations interacting with phonons, i.e. the phonon wind, the Hamiltonian of interest consists of a sum of two terms

$$H = H_{\mathrm{ph}} + H_{\mathrm{int}}(t) \tag{4.3}$$

where H_{ph} is the free phonon contribution while $H_{\mathrm{int}}(t)$ is the time-dependent interaction Hamiltonian between the phonons and the moving dislocation. In the following we will denote the dislocation wave vector by $\mathbf{q}$ (cf. previous section), whereas the phonon momenta will be $\mathbf{q}'$, $\mathbf{q}''$.

In the continuum limit where the lattice spacing goes to zero, the discrete sum over momenta may be replaced by an integral over the first Brillouin zone (BZ). Thus

$$H_{\rm ph} \to \frac{\hbar}{2} \sum_s \int \frac{d^3\mathbf{q}'}{(2\pi)^3}\, \omega_s(\mathbf{q}') \left(\hat{a}_s^\dagger(\mathbf{q}')\, \hat{a}_s(\mathbf{q}') + \hat{a}_s(\mathbf{q}')\, \hat{a}_s^\dagger(\mathbf{q}') \right) \tag{4.4}$$

where the quantized phonon mode creation and destruction operators obey the commutation relation (2.28), in the continuous momentum variables, presently denoted $\mathbf{q}'$, $\mathbf{q}''$.

The interaction Hamiltonian $H_{\rm int}$ may be obtained from eq. (2.29) by reinterpreting the displacements as superpositions of phonons and displacements due to a moving dislocation. For the displacement gradients appearing in $\mathcal{U}_3$ this means $u_{i,j} \to U_{i,j} = u_{i,j} + d_{i,j}$, and

$$d_{i,j}(\mathbf{x}, t) = \int \frac{d^3\mathbf{q}}{(2\pi)^3} \bar{d}_{i,j}(\mathbf{q}) \exp\left\{ i\mathbf{q} \cdot (\mathbf{x} - \mathbf{v}t) \right\} \tag{4.5}$$

where $\bar{d}_{i,j}(\mathbf{q})$ is the Fourier transform of the static deformation field of the dislocation and $\mathbf{v}$ its velocity. We obtain the time-dependent interaction Hamiltonian by keeping those terms containing two displacement gradients due to phonons $u_{i,j}$ and one due to the dislocation:

$$\begin{aligned} H_{\rm int}(t) &= \frac{1}{2!} \sum_{ijki'j'k'} D_{ijk}^{i'j'k'} \int d^3\mathbf{x}\, u_{i,i'}(\mathbf{x})\, u_{j,j'}(\mathbf{x})\, d_{k,k'}(\mathbf{x}, t) \\ &= \int d^3\mathbf{x} \Big\{ \left(\mathfrak{l} - \mathfrak{m} + \frac{\mathfrak{n}}{2} \right) (u_{i,i})^2 d_{k,k} + \frac{1}{2} \left(\mathfrak{m} - \frac{\mathfrak{n}}{2} + \lambda \right) (d_{i,i}\, u_{j,k}\, u_{j,k} + 2 u_{i,i}\, u_{j,k}\, d_{j,k}) \\ &\quad + \frac{1}{2} \left(\mathfrak{m} - \frac{\mathfrak{n}}{2} \right) (d_{i,i}\, u_{j,k}\, u_{k,j} + 2 u_{i,i}\, u_{j,k}\, d_{k,j}) + \frac{\mathfrak{n}}{4}\, u_{i,j}\, u_{j,k}\, d_{k,i} \\ &\quad + \left(\frac{\mathfrak{n}}{4} + \mu \right) (d_{i,j}\, u_{i,k}\, u_{k,j} + u_{i,j}\, d_{i,k}\, u_{k,j} + u_{i,j}\, u_{i,k}\, d_{k,j}) \Big\}. \end{aligned} \tag{4.6}$$

with elastic constants following from (2.31), (2.32), (2.33), and (2.34). The elastic deformation fields are given in terms of the phonon modes (2.27) by

$$u_{i,j}(\mathbf{x}) = i \sqrt{\frac{\hbar}{2\rho_0}} \sum_s \int \frac{d^3\mathbf{q}'}{(2\pi)^3} \frac{1}{\sqrt{\omega_s(\mathbf{q}')}} \left(\hat{a}_s(\mathbf{q}') + \hat{a}_s^\dagger(-\mathbf{q}') \right) e^{i\mathbf{q}'\cdot\mathbf{x}}\, q'_j\, \mathrm{e}_i(\mathbf{q}', s) \tag{4.7}$$

in the continuum limit of an infinite crystal, where ρ_0 is its mass density and $\mathrm{e}_i(\mathbf{q}', s)$ is the polarization vector of the elastic deformation.

Substituting these relations into (4.6) and noting that the integration over $\mathbf{x}$ gives a momentum conserving δ-function which sets $\mathbf{q}'' = \mathbf{q}' - \mathbf{q}$ (upon flipping the sign of $\mathbf{q}'$ under the integral), we secure

$$H_{\rm int}(t) = \sum_{ss'} \int \frac{d^3\mathbf{q}'}{(2\pi)^3} \int \frac{d^3\mathbf{q}}{(2\pi)^3}\, \xi_s^\dagger(\mathbf{q}')\, \xi_{s'}(\mathbf{q}' - \mathbf{q})\, \Gamma_{ss'}(\mathbf{q}', \mathbf{q}' - \mathbf{q})\, e^{-i\mathbf{q}\cdot\mathbf{v}t} \tag{4.8}$$

where

$$\begin{aligned} \Gamma_{ss'}(\mathbf{q}', \mathbf{q}' - \mathbf{q}) &= \frac{\hbar}{4\rho_0} \frac{1}{\sqrt{\omega_s(\mathbf{q}')\, \omega_{s'}(\mathbf{q}' - \mathbf{q})}} \\ &\quad \times \sum_{ijki'j'k'} D_{ijk}^{i'j'k'}\, q'_{i'} (q' - q)_{j'} \mathrm{e}_i^*(\mathbf{q}', s) \mathrm{e}_j(\mathbf{q}' - \mathbf{q}, s')\, \bar{d}_{kk'}(\mathbf{q}) \end{aligned} \tag{4.9}$$

is the vertex describing the interaction between the dislocation and the phonon modes. We have also defined

$$\xi_s(\mathbf{q}') \equiv \hat{a}_s(\mathbf{q}') + \hat{a}_s^\dagger(-\mathbf{q}') = \xi_s^\dagger(-\mathbf{q}') \tag{4.10}$$

and used $\omega_s(-\mathbf{q}') = \omega_s(\mathbf{q}')$ and (2.26) in arriving at (4.8).

Note that the form of Γ in (4.9) coincides (up to notation) with the one given in Ref. [22] (see also [23–25] for earlier work on phonon wind). Since the vast majority of high-rate plastic flow calculations are performed for temperatures on the order of and higher than the Debye temperature, we neglect here the so-called flutter effect which is important only at low temperatures; see [21] for details.

We choose coordinates so that edge and screw dislocations are along the z-axis and the dislocations move with speed v in the x-direction. Thus the glide plane for edge dislocations will be the x-z plane and we can write

$$\bar{d}_{i,j}(\mathbf{q}) = 2\pi\delta(q_z)\tilde{d}_{i,j}(q,\phi) \tag{4.11}$$

with $\mathbf{q} = q(\cos\phi, \sin\phi, 0)$. Explicit expressions for the two-dimensional deformation fields $\tilde{d}_{ij}(q,\phi)$ of edge and screw dislocations are given in Section 3, cf. eqs. (3.10), (3.12).

Since the phonon wave vectors lie in the first Brillouin zone, $|\mathbf{q}'|$, $|\mathbf{q}''| \leq q_{\mathrm{BZ}}$, the dislocation wave vector magnitude satisfies $q = |\mathbf{q}' - \mathbf{q}''| \leq 2q_{\mathrm{BZ}}$ due to momentum conservation. The coefficients $D_{ijk}^{i'j'k'}$ depend on second- and third-order elastic constants as explained in Section 2.3. Finally, we introduce the following short hand notation: $\omega_s(q') \to \omega_{q'}$, $\mathrm{e}_i(q',s) \to \mathrm{e}_{q'i}$, $\xi_{\mathbf{q}'s} \to \xi_{q'}$ with $\xi_{\mathbf{q}'s} = \hat{a}_{\mathbf{q}'s} + \hat{a}^\dagger_{-\mathbf{q}'s}$, and $\Gamma_{q'q''} \equiv \Gamma_{s's''}(\mathbf{q}',\mathbf{q}'')$, i.e. in order to write equations more compactly we use "superindices" q for the dependence on the polarization and the 3-momenta. Note that the polarization indices are implicit. In the following we will denote phonon momenta by $\mathbf{q}'$ and $\mathbf{q}''$ while the momentum of a dislocation will be denoted by $\mathbf{q}$.

We now derive an expression for the dissipation D starting from the probability per unit time of scattering a phonon from state q' to state q'' [22, 26], $W_{q'q''} = \frac{8\pi}{\hbar^2}|\Gamma_{q'q''}|^2\delta(\omega_{q'} - \omega_{q''} - \Omega_q)$, where $\Gamma_{q'q''}$ is the dislocation-phonon vertex defined in (4.9) and $\Omega_q = \mathbf{q}\cdot\mathbf{v}$. Multiplying $W_{q'q''}$ by $n_{q'} = (\exp(\hbar\omega_{q'}/k_BT) - 1)^{-1}$, the equilibrium phonon distribution function, gives the number of transitions per unit time. Taking into account that an energy $\hbar(\omega_{q'} - \omega_{q''}) = \hbar\Omega_q$ is transferred for every transition, one finds for the dissipation (energy dissipated per unit time per unit length of a dislocation)

$$\begin{aligned} D &= -\frac{8\pi}{\hbar}\sum_{q',q''}\Omega_q|\Gamma_{q'q''}|^2 n_{q'}\delta(\omega_{q'} - \omega_{q''} - \Omega_q) \\ &= \frac{4\pi}{\hbar}\sum_{q',q''}\Omega_q|\Gamma_{q'q''}|^2(n_{q''} - n_{q'})\delta(\omega_{q'} - \omega_{q''} - \Omega_q)\,, \end{aligned} \tag{4.12}$$

where momentum conservation $\mathbf{q} = \mathbf{q}' - \mathbf{q}''$ is implicit so as to avoid clutter in the notation. The same expression can be derived from the one-loop Feynman diagram depicted in Figure 3; see [25] for details. Since Ω_q is already linear in the dislocation velocity, $\lim_{v\to 0}\Gamma_{q'q''}$ may be considered as a lowest-order approximation for very small velocities. Indeed, this is what Al'shits et al. consider in Ref. [22], computing Γ for a straight line and loop dislocation at zero velocity and for an isotropic crystal; see also the review article [21]. Here we aim at pushing to higher velocities and hence must use a v-dependent $\Gamma_{q'q''}$, i.e. eq. (4.9) with the displacement gradients of (3.10), (3.12). For the elastic constants $D_{ijk}^{i'j'k'}$ we will, for now, use experimental values rather

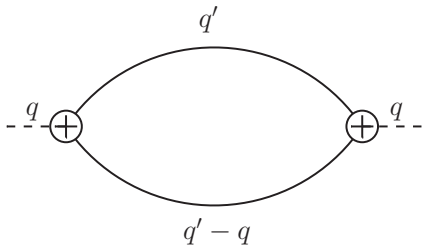

Figure 3: The lowest order Feynman graph describing phonon wind: The top and bottom lines represent phonon propagators with momenta $\mathbf{q}'$ and $\mathbf{q}'' = \mathbf{q}' - \mathbf{q}$ respectively. The vertices left and right depend on the phonon and dislocation wave vectors and are presently denoted by $\Gamma_{q'q''}$.

than compute them from the crystal potential. In particular, we will specialize to the isotropic approximation in the next section.

From (4.12) we obtain the drag coefficient for phonon wind in the continuum approximation[3]

$$B = D/v^2 = \frac{4\pi}{\hbar v^2} \int_0^{q_{\rm BZ}} \frac{dq'\, q'^2}{(2\pi)^3} \int_{-1}^{1} d\cos\theta' \int_0^{2\pi} d\phi' \int_0^{2q_{\rm BZ}} \frac{dq\, q}{(2\pi)^2} \int_0^{2\pi} d\phi\; \Omega_q |\Gamma_{q',q'-q}(q,\phi)|^2 (n_{q'-q} - n_{q'}) \\ \times \delta(\omega_{q'} - \omega_{q'-q} - \Omega_q)\,, \tag{4.13}$$

with $\Omega_q = qv|\cos\phi|$ and $n_q = (\exp(\hbar\omega_q/k_BT) - 1)^{-1}$. Once more, we have approximated the sum over $\mathbf{q}'$ by an integral over the first Brillouin zone, i.e.

$$\sum_{\mathbf{q}'} \to V \int_{\rm BZ} \frac{d^3\mathbf{q}'}{(2\pi)^3}\,, \tag{4.14}$$

and subsequently expressed $\mathbf{q}'$ in spherical coordinates: $\mathbf{q}' = q'(\sin\theta'\cos\phi'\hat{\mathbf{e}}_1 + \sin\theta'\sin\phi'\hat{\mathbf{e}}_2 + \cos\theta'\hat{\mathbf{e}}_3)$. Then choosing these coordinates such that θ' is the angle from the direction of $\mathbf{q}$, we have

$$(\mathbf{q}' - \mathbf{q}\,)^2 = q^2 + q'^2 - 2qq'\cos\theta'\,, \tag{4.15}$$

and the delta function can be used to perform the integral over θ', since $\omega_{q'-q}$ is a function of $|\mathbf{q}' - \mathbf{q}\,|$. This implies $\hat{\mathbf{e}}_3 = \mathbf{q}/q$, and the basis vectors $\hat{\mathbf{e}}_{1,2,3}$ are therefore related to the Cartesian ones via

$$\hat{\mathbf{e}}_3 = \cos\phi\,\hat{\mathbf{x}} + \sin\phi\,\hat{\mathbf{y}}\,, \qquad \hat{\mathbf{e}}_1 = -\sin\phi\,\hat{\mathbf{x}} + \cos\phi\,\hat{\mathbf{y}}\,, \qquad \hat{\mathbf{e}}_2 = \hat{\mathbf{z}}\,, \tag{4.16}$$

[3] The integration of q ranges up to infinity because we modeled our dislocations in the continuum limit. However, the integration range reduces to a finite value ($q \le 2q_{\rm BZ}$) by the momentum conserving delta function because the magnitudes of the phonon wave vectors q', q'' are limited to the first Brillouin zone, see also Ref. [22]. Another subtlety concerns Ω_q: Alshits defined this quantity without the absolute value. However, negative values merely correspond to incoming and outgoing phonons exchanging their meaning and with some variable substitutions under the integrals it is fairly easy to show that both cases, $\cos\phi > 0$, $\cos\phi < 0$, can be combined into our expression (4.13).

leading to

$$\mathbf{q}' = q' \begin{pmatrix} \cos\theta' \cos\phi - \sin\theta' \cos\phi' \sin\phi \\ \cos\theta' \sin\phi + \sin\theta' \cos\phi' \cos\phi \\ \sin\theta' \sin\phi' \end{pmatrix}, \quad \mathbf{q}' - \mathbf{q} = q' \begin{pmatrix} (\cos\theta' - \frac{q}{q'}) \cos\phi - \sin\theta' \cos\phi' \sin\phi \\ (\cos\theta' - \frac{q}{q'}) \sin\phi + \sin\theta' \cos\phi' \cos\phi \\ \sin\theta' \sin\phi' \end{pmatrix}, \tag{4.17}$$

which is clearly consistent with (4.15). We are now able to construct the corresponding polarization vectors, keeping in mind that the longitudinal polarizations are unit vectors parallel to the respective momenta. Another useful relation which follows from completeness of the polarization vectors, $\sum_s \mathrm{e}_i^*(\mathbf{q}', s)\mathrm{e}_j(\mathbf{q}', s) = \delta_{ij}$, is:

$$\begin{aligned} \sum_{s=1,2} \mathrm{e}_i^*(\mathbf{q}', s)\mathrm{e}_j(\mathbf{q}', s) &= \delta_{ij} - \frac{q_i' q_j'}{q'^2}\,, \\ \sum_{s=1,2} \mathrm{e}_i^*(\mathbf{q}' - \mathbf{q}, s)\mathrm{e}_j(\mathbf{q}' - \mathbf{q}, s) &= \delta_{ij} - \frac{(q_i' - q_i)(q_j' - q_j)}{(\mathbf{q}' - \mathbf{q})^2}\,, \end{aligned} \tag{4.18}$$

where we have chosen $s = 1, 2$ as the transverse polarizations. We thus find for $|\Gamma_{q',q'-q}|^2$ the expression

$$\begin{aligned} |\Gamma_{q',q'-q}(q,\phi)|^2 = \frac{\hbar^2}{16\rho_0^2 \omega_{q'}\omega_{q'-q}} \sum_{\substack{i,i',j,j',k,k' \\ l,m,n,l',m',n'}} & \tilde{d}_{k,k'}(q,\phi)\tilde{d}_{n,n'}(q,\phi) q_{i'}' q_{l'}' (q'-q)_{j'}(q'-q)_{m'} \\ & \times \mathrm{e}_i^*(\mathbf{q}', s')\mathrm{e}_j(\mathbf{q}' - \mathbf{q}, s'')\mathrm{e}_l(\mathbf{q}', s')\mathrm{e}_m^*(\mathbf{q}' - \mathbf{q}, s'') D_{ijk}^{i'j'k'} D_{lmn}^{l'm'n'}\,, \end{aligned} \tag{4.19}$$

where all sums go over x, y, z, although depending on whether an edge or a screw dislocation is considered, different components of the deformation fields vanish, see Eqns. (3.10), (3.12).

In order to perform the integral over θ' using the delta function, we make the following variable substitution:

$$W(q, q', \theta') = \omega_{q'-q} = \omega_{s''}(q^2 + q'^2 - 2qq'\cos\theta')\,, \qquad dW = \frac{\partial W}{\partial \cos\theta'} d\cos\theta'\,. \tag{4.20}$$

In addition, θ' appearing in the Jacobi determinant and in the kinematic factors (4.19) is replaced by the inverse function $\theta'(q, q', W)$, assuming it exists. For the drag coefficient, this leads to

$$\begin{aligned} B = \frac{\hbar\pi}{4\rho_0^2} \int_0^{q_{\mathrm{BZ}}} \frac{dq'\, q'^2}{(2\pi)^3} \int_0^{2q_{\mathrm{BZ}}} \frac{dq\, q^2}{(2\pi)^2} \int_0^{2\pi} d\phi \frac{\cos\phi}{v\,\omega_{q'}(\omega_{q'} - \Omega_q)} \left(\left(e^{\frac{\hbar(\omega_{q'} - \Omega_q)}{k_{\mathrm{B}}T}} - 1 \right)^{-1} - \left(e^{\frac{\hbar\omega_{q'}}{k_{\mathrm{B}}T}} - 1 \right)^{-1} \right) \\ \times \int_{W_{\max}}^{W_{\min}} dW \left(\frac{\partial W}{\partial \cos\theta'} \right)^{-1} \delta(\omega_{q'} - \Omega_q - W) \sum_{\substack{i,i',j,j',k,k' \\ l,m,n,l',m',n'}} \mathrm{e}_i^*(\mathbf{q}', s')\mathrm{e}_j(\mathbf{q}' - \mathbf{q}, s'')\mathrm{e}_l(\mathbf{q}', s') \\ \times \mathrm{e}_m^*(\mathbf{q}' - \mathbf{q}, s'') D_{ijk}^{i'j'k'} D_{lmn}^{l'm'n'} \tilde{d}_{k,k'}(q,\phi)\tilde{d}_{n,n'}(q,\phi) \int_0^{2\pi} d\phi'\, q_{i'}' q_{l'}' (q'-q)_{j'}(q'-q)_{m'}\,, \end{aligned} \tag{4.21}$$

where $W_{\max} = \omega_{s''}((\mathbf{q}+\mathbf{q}')^2)$, $W_{\min} = \omega_{s''}((\mathbf{q}-\mathbf{q}')^2)$. Note that the only ϕ'-dependence in (4.13) comes from the kinematic factors in (4.19). Thus the ϕ'-integral is independent of the dispersion

relation and can be done explicitly, as it is of the type

$$\int_0^{2\pi} d\phi' \sin^m \phi' \cos^n \phi' \tag{4.22}$$

with $m, n \geq 0$ and $m + n \leq 8$ for all terms (since ϕ' appears only within components of vector q_i' and the polarization vectors, each of which in turn appear at most to fourth power).

4.2 Interaction with Transverse and Longitudinal Phonons

In the isotropic case, we have the elastic constants of the form given in Section 2.3. For the frequencies we then have three modes, one longitudinal, $\omega_{\mathrm{L}}(q)$, and two transverse, $\omega_{\mathrm{T}}(q)$. In the continuum limit one may approximate these modes as

$$\omega_{\mathrm{L}}(q) \approx c_{\mathrm{L}}|\mathbf{q}| = |\mathbf{q}|\sqrt{(\lambda + 2\mu)/\rho_0}\,, \qquad \omega_{\mathrm{T}}(q) \approx c_{\mathrm{T}}|\mathbf{q}| = |\mathbf{q}|\sqrt{\mu/\rho_0}\,. \tag{4.23}$$

The underlying lattice is taken into account indirectly by cutting off the spectrum at some limiting frequency (typically the Debye frequency) which is related to the finite lattice spacing. One obvious shortcoming of this approximation (apart being a very crude linear approximation of a more complicated spectrum dependent on the crystal structure), is that its derivative at the zone boundary does not vanish; hence, it is a poor approximation to the true phonon spectrum at high frequencies. Some improvement might be achieved by employing a sine function [27] instead of this linear relation. However, in order to be consistent with the continuum approximation, we will for now only consider the simplest case of the Debye approximation (4.23), leaving a more thorough study of dispersion relations and their effect on the predictions for the drag coefficient to future work.

Using the delta function (but not yet for integration), we may replace all occurrences of $\omega_{q'-q}$ in eq. (4.13) with $\omega_{q'} - \Omega_q$ in the integrand so that the only dependence on θ' is in the q_i' (and related polarization vectors) with indices contracted with the elastic constants. Furthermore, with $s = 1,2,3$ and $c_1 = c_2 = c_{\mathrm{T}}$, $c_3 = c_{\mathrm{L}}$, $\omega_1(q) = \omega_2(q) = \omega_{\mathrm{T}}(q)$, and $\omega_3(q) = \omega_{\mathrm{L}}(q)$, we have [4]

$$\begin{aligned}\delta(\omega_{s'}(q') - \omega_{s''}(|\mathbf{q}' - \mathbf{q}|) - \Omega_q) = {} & \delta\left(\cos\theta' - \frac{1}{2c_{s''}^2 qq'}\left((c_{s''}^2 q^2 + (c_{s''}^2 - c_{s'}^2)q'^2 + 2c_{s'}q'\Omega_q - \Omega_q^2\right)\right) \\ & \times \frac{|c_{s'}q' - \Omega_q|}{c_{s''}^2 qq'}\Theta\left(2c_{s''}^2 qq' - \left|(c_{s''}^2 q^2 + (c_{s''}^2 - c_{s'}^2)q'^2 + 2c_{s'}q'\Omega_q - \Omega_q^2\right|\right)\,,\end{aligned} \tag{4.24}$$

where $\Theta(x)$ is the step function following from $\cos\theta' \in [-1, 1]$. (Here, it is of course trivially 1 due to the delta function, but after the integration over $\cos\theta'$ it needs to be taken into account.) This allows us to easily integrate $\cos\theta'$ in the expression for B, and the step function can subsequently be translated into integral boundaries for the q integration. Furthermore, according to the delta function above, $\omega_{s'}(q') - \Omega_q = \omega_{s''}(|\mathbf{q}' - \mathbf{q}|) \geq 0$. In the case where $s' = s''$, this expression simplifies considerably leading to

$$\begin{aligned}\delta(\omega_s(q') - \omega_s(|\mathbf{q}' - \mathbf{q}|) - \Omega_q) = {} & \frac{|c_s q' - \Omega_q|}{c_s^2 qq'}\,\delta\left(\cos\theta' - \frac{1}{2c_s^2 qq'}\left((c_s^2 q^2 + 2c_s q'\Omega_q - \Omega_q^2\right)\right) \\ & \times \Theta\left(2c_s^2 qq' - \left|(c_s^2 q^2 + 2c_s q'\Omega_q - \Omega_q^2\right|\right)\,,\end{aligned} \tag{4.25}$$

[4] Note that eq. (4.24) is valid only for the linear dispersion relation $\omega_s(q) \approx c_s|\mathbf{q}|$.

and some algebra finally leads to $(\cos\theta' - (v/c_s)|\cos\phi)| \geq 0$, which further restricts the ranges of the contributing angles. It has indeed been argued [22, 28] that the purely transverse yield the dominating contribution at low velocities. Naively, this argument is based on the fact that at low velocities, inverse powers of sound speed in the full expression lead to a suppression of the longitudinal modes. We will verify this claim also for high velocities below.

Whenever $s' = s''$ it will be convenient [5] to change variables from q to the dimensionless variable t:

$$\begin{aligned} t &= \frac{1}{2c_s^2 q q'}\left((c_s^2 q^2 + 2c_s q'\Omega_q - \Omega_q^2\right) = \frac{1}{2q'}\left(1-\beta_s^2\cos^2\phi\right) q + \beta_s|\cos\phi|\,, \\ dt &= \frac{1}{2q'}\left(1-\beta_s^2\cos^2\phi\right) dq\,, \qquad\qquad t \in [\beta_s|\cos\phi|, 1]\ . \end{aligned} \tag{4.26}$$

We have assumed a dislocation velocity below transverse sound speed, i.e. $v < c_\mathrm{T} < c_\mathrm{L}$, and therefore $\beta_s = v/c_s < 1$ $(s = 1, 2, 3)$. The upper bound $(t \leq 1)$ is due to the step function above. Note that the delta function in (4.25) and the definition of t imply $\cos\theta' = t$.

Considering first the purely transverse modes and introducing unit vectors $\hat{q}_i = q_i/q$, $\hat{q}'_i = q'_i/q'$, our isotropic drag coefficient reads [6]

$$\begin{aligned} B = {} & \frac{\pi\hbar}{4\rho_0^2 v c_\mathrm{T}^3}\int_0^{q_\mathrm{BZ}}\frac{dq'}{(2\pi)^3}\int_0^{2\pi}d\phi\int_0^{2q_\mathrm{BZ}}\frac{dq\,q}{(2\pi)^2}|\cos\phi|\left(\frac{1}{e^{\frac{\hbar}{k_\mathrm{B}T}c_\mathrm{T}q'}-1} - \frac{1}{e^{\frac{\hbar}{k_\mathrm{B}T}(c_\mathrm{T}q' - vq|\cos\phi|)}-1}\right) \\ & \times \sum_{\substack{i,i',j,j',k,k' \\ l,m,n,l',m',n'}} \tilde{d}_{k,k'}(q,\phi)\tilde{d}_{n,n'}(q,\phi)\int_0^{2\pi}d\phi'\int_{-1}^{1}d\cos\theta'\, q'_{i'}q'_{l'}(q'-q)_{j'}(q'-q)_{m'}D_{ijk}^{i'j'k'}D_{lmn}^{l'm'n'} \\ & \times \left(\delta_{il} - \frac{q'_i q'_l}{q'^2}\right)\left(\delta_{jm} - \frac{(q'_j - q_j)(q'_m - q_m)}{(\mathbf{q}'-\mathbf{q}\,)^2}\right)\delta\big(\cos\theta' - t(q)\big) \\ = {} & \frac{\pi\hbar}{2\rho_0^2}\int_0^{q_\mathrm{BZ}}\frac{dq'\,q'^6}{(2\pi)^5}\int_0^{2\pi}d\phi\int_{\beta_\mathrm{T}|\cos\phi|}^{1}dt\;\tilde{q}|\cos\phi|\left(\frac{1}{e^{\frac{\hbar c_\mathrm{T}}{k_\mathrm{B}T}q'}-1} - \frac{1}{e^{\frac{\hbar c_\mathrm{T}}{k_\mathrm{B}T}q'(1-\beta_\mathrm{T}\tilde{q}|\cos\phi|)}-1}\right) \\ & \times \sum_{\substack{i,i',j,j',k,k' \\ l,m,n,l',m',n'}} \frac{\tilde{d}_{k,k'}(q,\phi)\tilde{d}_{n,n'}(q,\phi)}{\beta_\mathrm{T}c_\mathrm{T}^4\left(1-\beta_\mathrm{T}^2\cos^2\phi\right)}\int_0^{2\pi}d\phi'\,\hat{q}'_{i'}\hat{q}'_{l'}\left(\hat{q}'_{j'}\hat{q}'_{m'} - \tilde{q}\,\hat{q}_{j'}\hat{q}'_{m'} - \tilde{q}\,\hat{q}'_{j'}\hat{q}_{m'} + \tilde{q}^2\,\hat{q}_{j'}\hat{q}_{m'}\right) \\ & \times (\delta_{il} - \hat{q}'_i\hat{q}'_l)\left(\delta_{jm} - \frac{(\hat{q}'_j - \tilde{q}\hat{q}_j)(\hat{q}'_m - \tilde{q}\hat{q}_m)}{1+\tilde{q}^2 - 2t\tilde{q}}\right)D_{ijk}^{i'j'k'}D_{lmn}^{l'm'n'}, \end{aligned} \tag{4.27}$$

where we have eliminated q in favor of the dimensionless variable t:

$$\tilde{q} := \frac{q(t)}{q'} = \frac{2}{\left(1-\beta_\mathrm{T}^2\cos^2\phi\right)}\left(t - \beta_\mathrm{T}|\cos\phi|\right)\ . \tag{4.28}$$

[5] In fact, this variable substitution is only useful for the simplest case of a linear dispersion relation, and only if the interaction is with purely transverse (or longitudinal) phonons, but not mixed.

[6] The integration range of q is further restricted by the remaining delta function together with the range of $\cos\theta'$, in particular $q \leq 2q_\mathrm{BZ}/(1+\beta_s\cos\phi)$ if $\cos\phi > 0$ and $q \leq 2q_\mathrm{BZ}$ otherwise. In the limit of zero dislocation velocity, the integration range of q remains unchanged, i.e. $q \leq 2q_\mathrm{BZ}$ — cf. [22].

Since $\cos\theta' = t$ the components of the unit vector $\hat{q}'_i = q'_i/q'$ depend on t

$$\hat{q}'_i = \begin{pmatrix} t\cos\phi - \sqrt{1-t^2}\sin\phi\cos\phi' \\ t\sin\phi + \sqrt{1-t^2}\cos\phi\cos\phi' \\ \sqrt{1-t^2}\sin\phi' \end{pmatrix} . \tag{4.29}$$

As remarked earlier, the integral over ϕ' can also be done easily; see (4.22).

Due to the appearance of the two transverse projection operators in the last line of (4.27), $3a = \mathfrak{l} - \mathfrak{m} + \frac{\mathfrak{n}}{2}$ does not contribute to the interaction with purely transverse phonons. The reason is that this term parametrizes three traces, $a\delta_{ii'}\delta_{jj'}\delta_{kk'}$, leading to expressions like $q'_i(\delta_{il} - \hat{q}'_i\hat{q}'_l) = 0$, see (2.31), (4.6). For the same reason, most terms proportional to $\tilde{b} = \mathfrak{m} - \frac{\mathfrak{n}}{2}$ and λ (see (4.6), (2.32) and (2.18)) drop out as well, the only surviving ones being those where the trace, $\delta_{kk'}$, hits an edge dislocation since $\tilde{d}_{ii}$ is nonzero only in the edge case, see (3.11). For these reasons, the drag coefficient for screw dislocations interacting with purely transverse phonons depends only on the two elastic constants μ, $\mathfrak{n}$, whereas dislocation drag for edge dislocations interacting with purely transverse phonons depends on the four elastic constants λ, μ, $\mathfrak{m}$, and $\mathfrak{n}$.

If we insert eq. (3.10) or (3.12) for the displacement gradients (and hence neglect any cutoffs), we observe that $q'^2\tilde{d}_{k,k'}(q,\phi)\tilde{d}_{n,n'}(q,\phi) = \tilde{d}_{k,k'}(\tilde{q},\phi)\tilde{d}_{n,n'}(\tilde{q},\phi)$, allowing us to evaluate the integral over q' in terms of Debye functions [29, 30]. These are defined as

$$D_n(x) = \int_0^x \frac{y^n}{e^y - 1} dy = x^n \left(\frac{1}{n} - \frac{x}{2(n+1)} + \sum_{k=1}^{\infty} \frac{B_{2k} x^{2k}}{(2k+n)(2k)!} \right) , \tag{4.30}$$

where $|x| < 2\pi$, $n \geq 1$, and the coefficients B_{2k} are Bernoulli numbers[7]. In particular we have

$$\begin{aligned} &\int_0^{q_{\mathrm{BZ}}} dq'\, q'^4 \left(\frac{1}{e^{\frac{\hbar c_{\mathrm{T}}}{k_{\mathrm{B}}T} q'} - 1} - \frac{1}{e^{\frac{\hbar c_{\mathrm{T}}}{k_{\mathrm{B}}T} q'(1-\beta_{\mathrm{T}}\tilde{q}|\cos\phi|)} - 1} \right) \\ &= \left(\frac{k_{\mathrm{B}}T}{\hbar c_{\mathrm{T}}} \right)^5 \left(D_4\Big(\tfrac{\hbar c_{\mathrm{T}}}{k_{\mathrm{B}}T} q_{\mathrm{BZ}}\Big) - \frac{D_4\Big(\tfrac{\hbar c_{\mathrm{T}}}{k_{\mathrm{B}}T}(1-\beta_{\mathrm{T}}\tilde{q}|\cos\phi|) q_{\mathrm{BZ}}\Big)}{(1-\beta_{\mathrm{T}}\tilde{q}|\cos\phi|)^5} \right) \\ &= \left(\frac{k_{\mathrm{B}}T}{2\hbar c_{\mathrm{T}}} \right) (q_{\mathrm{BZ}})^4 \sum_{k=0}^{\infty} \frac{B_{2k} \left(\frac{\hbar c_{\mathrm{T}}}{k_{\mathrm{B}}T} q_{\mathrm{BZ}} \right)^{2k} \Big(1 - (1-\beta_{\mathrm{T}}\tilde{q}|\cos\phi|)^{2k-1} \Big)}{(k+2)(2k)!} . \end{aligned} \tag{4.31}$$

The series representation of these Debye functions converges only for $\hbar c_{\mathrm{T}} q_{\mathrm{BZ}} < 2\pi k_{\mathrm{B}}T$, which is automatically fulfilled if T is greater than the Debye temperature.

Taking only the leading order term of (4.31), we then find for the drag coefficient in the high temperature limit

$$\begin{aligned} B \approx\; & \frac{\pi k_{\mathrm{B}}T}{8\rho_0^2} \frac{(q_{\mathrm{BZ}})^4}{(2\pi)^5} \int_0^{2\pi} d\phi \int_{\beta_{\mathrm{T}}|\cos\phi|}^1 dt\, \frac{\tilde{q}^2\cos^2\phi}{(1-\beta_{\mathrm{T}}\tilde{q}|\cos\phi|)} \\ & \times \sum_{\substack{i,i',j,j',k,k' \\ l,m,n,l',m',n'}} \frac{\tilde{d}_{k,k'}(\tilde{q},\phi)\tilde{d}_{n,n'}(\tilde{q},\phi)}{c_{\mathrm{T}}^5 \left(1-\beta_{\mathrm{T}}^2\cos^2\phi\right)} \int_0^{2\pi} d\phi'\, \hat{q}'_{i'}\hat{q}'_{l'} \left(\hat{q}'_{j'}\hat{q}'_{m'} - \tilde{q}\,\hat{q}_{j'}\hat{q}'_{m'} - \tilde{q}\,\hat{q}'_{j'}\hat{q}_{m'} + \tilde{q}^2\,\hat{q}_{j'}\hat{q}_{m'} \right) \\ & \times (\delta_{il} - \hat{q}'_i\hat{q}'_l) \left(\delta_{jm} - \frac{(\hat{q}'_j - \tilde{q}\hat{q}_j)(\hat{q}'_m - \tilde{q}\hat{q}_m)}{(1-\beta_{\mathrm{T}}\tilde{q}|\cos\phi|)^2} \right) D_{ijk}^{i'j'k'} D_{lmn}^{l'm'n'} + \mathcal{O}(1/(k_{\mathrm{B}}T)) . \end{aligned} \tag{4.32}$$

[7] The first four appearing in the sum of eq. (4.31) are $B_0 = 1$, $B_2 = 1/6$, $B_4 = -1/30$, and $B_6 = 1/42$.

However, since we are interested in room temperature which is of the same order of magnitude as the Debye temperature for many materials, we will perform the q' integral numerically, giving us better accuracy.

Before we do so, however, let us briefly remark on the limit $v \to 0$, as this limit allows us to compare to earlier work. In this case $\tilde{q} \to 2t$, according to (4.28), which leads to

$$\begin{aligned}\lim_{v\to 0} B \approx \frac{\pi k_{\mathrm{B}} T}{8\rho_0^2}\frac{(q_{\mathrm{BZ}})^4}{(2\pi c_{\mathrm{T}})^5}\int_0^{2\pi} d\phi \int_0^1 dt\ \cos^2\phi \\ \times \sum_{\substack{i,i',j,j',k,k'\\ l,m,n,l',m',n'}} \lim_{v\to 0}\tilde{d}_{k,k'}(1,\phi)\tilde{d}_{n,n'}(1,\phi)\int_0^{2\pi} d\phi'\ \hat{q}'_{i'}\hat{q}'_{l'}(\hat{q}'_{j'}-2t\hat{q}_{j'})(\hat{q}'_{m'}-2t\hat{q}_{m'}) \\ \times (\delta_{il}-\hat{q}'_i\hat{q}'_l)\left(\delta_{jm}-(\hat{q}'_j-2t\hat{q}_j)(\hat{q}'_m-2t\hat{q}_m)\right) D^{i'j'k'}_{ijk} D^{l'm'n'}_{lmn} + \mathcal{O}(1/(k_{\mathrm{B}}T))\,, \end{aligned} \tag{4.33}$$

and inserting the zero velocity limits of the dislocation displacement gradients of Section 3 (with magnitudes q replaced by 1), the expression above can be easily integrated analytically, since upon substituting $t = \cos\theta'$ all three remaining integrals only involve powers of sine and cosine (see (4.29)). We will come back to this point later where we will also include next to leading order terms.

Next, consider the drag coefficient (again in the high temperature expansion) for the interaction of dislocations with purely longitudinal phonons. In this case, (4.32) is replaced by

$$\begin{aligned} B \approx \frac{\pi k_{\mathrm{B}} T}{8\rho_0^2}\frac{(q_{\mathrm{BZ}})^4}{(2\pi)^5}\int_0^{2\pi} d\phi \int_{\beta_{\mathrm{L}}|\cos\phi|}^1 dt\ \frac{\tilde{q}^2\cos^2\phi}{(1-\beta_{\mathrm{L}}\tilde{q}|\cos\phi|)} \\ \times \sum_{\substack{i,i',j,j',k,k'\\ l,m,n,l',m',n'}} \frac{\tilde{d}_{k,k'}(\tilde{q},\phi)\tilde{d}_{n,n'}(\tilde{q},\phi)}{c_{\mathrm{L}}^5\,(1-\beta_{\mathrm{L}}^2\cos^2\phi)}\int_0^{2\pi} d\phi'\ \hat{q}'_{i'}\hat{q}'_{l'}\left(\hat{q}'_{j'}\hat{q}'_{m'}-\tilde{q}\,\hat{q}_{j'}\hat{q}'_{m'}-\tilde{q}\,\hat{q}'_{j'}\hat{q}_{m'}+\tilde{q}^2\,\hat{q}_{j'}\hat{q}_{m'}\right) \\ \times (\hat{q}'_i\hat{q}'_l)\left(\frac{(\hat{q}'_j-\tilde{q}\hat{q}_j)(\hat{q}'_m-\tilde{q}\hat{q}_m)}{(1-\beta_{\mathrm{L}}\tilde{q}|\cos\phi|)^2}\right) D^{i'j'k'}_{ijk} D^{l'm'n'}_{lmn} + \mathcal{O}(1/(k_{\mathrm{B}}T))\,, \end{aligned} \tag{4.34}$$

where now $\tilde{q} = q(t)/q' = 2\,(t-\beta_{\mathrm{L}}|\cos\phi|)\,/\,(1-\beta_{\mathrm{L}}^2\cos^2\phi)$. We see that, except inside the expressions for the dislocation displacement gradients, all c_{T} have been replaced by c_{L}, leading to the naive conclusion that due to the factor $1/c_{\mathrm{L}}^5$ the drag coefficient in the low-velocity regime is suppressed by $(c_{\mathrm{T}}/c_{\mathrm{L}})^5$, confirming what was pointed out in [28]. However, one must also take into account that other elastic constants are contributing due to the transverse polarization vectors being replaced by longitudinal ones, and this can offset the suppression. In the high velocity regime the divergent factor coming from the phonon distribution function also had its c_{T} dependence replaced by c_{L}, and thus we expect the transverse phonons to dominate as $v \to c_{\mathrm{T}}$. In particular, in going back to eq. (4.21) we notice that the phonon with polarization index s' is the one leading to divergent terms as $v \to c_{\mathrm{T}}$.

4.3 Drag Coefficient for $v \to c_{\mathrm{T}}$

The dominant terms in the drag coefficient as $v \to c_{\mathrm{T}}$ arise from

- the interaction with transverse phonons,

- elastic constants $\mathfrak{n}$ and μ since screw displacement gradients are traceless and the trace of the edge dislocation displacement gradient does not diverge as $v \to c_\mathrm{T}$, see (3.11),
- component $\tilde{d}_{z,x}$ in the screw case and $\tilde{d}_{y,x}$ in the edge case, the latter dominating over the former,
- and edge dislocations are more divergent in their displacement gradient field as $v \to c_\mathrm{T}$ than screw dislocations due to the above assessment, see (3.10), (3.12).

In eq. (4.27) (for $s = \mathrm{T}$) for the isotropic drag coefficient we see that the factor $1/(1 - \beta_\mathrm{T}^2 \cos^2\phi)$ diverges at $\cos\phi = \pm 1$ as β_T approaches 1. More powers of this factor come from the deformation fields (3.10) and (3.12). At the same time, the integration range of t shrinks to zero[8] obscuring the actual degree of divergence. In Appendix B we therefore analyze the divergence using an alternative set of variables. In the case of screw dislocations, the component $\tilde{d}_{z,y}$ does not contain a divergence due to the presence of γ_T^{-2}. Hence, in contrast to edge dislocations, screws only contribute factors of $\sin\phi/(1-\beta_\mathrm{T}^2\cos^2\phi)$ which diverge much slower than $\cos\phi/(1-\beta_\mathrm{T}^2\cos^2\phi)$ as $\phi \to 0$ (or π) and $\beta_\mathrm{T} \to 1$. Edge dislocations contribute both types of terms and hence lead to steeper curves as β_T approaches one.

The calculations of the drag coefficient for transverse phonons in Appendix B are carried out in Cartesian coordinates rather than in spherical coordinates. The focus is on the limiting behavior of B as $v \to c_\mathrm{T}$. In the case of screw dislocations scattering transverse phonons we conclude that the drag coefficient has no divergence and

$$B \propto \frac{b^2 k_\mathrm{B} T q_\mathrm{BZ}^4}{c_\mathrm{T}} \,. \tag{4.35}$$

In contrast, for the case of edge dislocations scattering transverse phonons the drag coefficient is divergent in the limit $v \to c_\mathrm{T}$ and

$$B \sim \frac{1}{\sqrt{1 - v^2/c_\mathrm{T}^2}} \,. \tag{4.36}$$

MD simulation results of Refs. [31, 32] indicate that screw dislocations can accelerate into the transonic regime, consistent with a convergent drag coefficient which we find here. Edge dislocations, on the other hand, can reach transonic speeds only by a "jump" according to those simulations. This jump indicates a sudden change, possibly in shape of the dislocation [33], and cannot be described by our present model of dislocation drag. Hence, the divergence we find here for B of edge dislocations only reflects the behavior prior to the observed jump into the transonic regime, i.e. where the dislocation velocity is still below transverse sound speed. Due to the limited resolution in the MD simulation results of [31, 32], it is as of yet unclear how close to the limiting velocity this jump happens [33].

A detailed stability analysis of dislocations in isotropic as well as cubic crystals was recently carried out [33]; in the isotropic limit an analytic line tension analysis showed that straight edge dislocations become unstable as they approach transverse sound speed. For this reason, as well as the fact that linear elasticity theory breaks down close to c_T (see Figures 1, 2), we show numerical results for the drag coefficient only up to 90% transverse sound speed in the next section.

Note that "relativistic" factors like $1/\left(1 - \beta_\mathrm{T}^2\right)^m$ with some exponent $1/2 \leq m \leq 4$ have appeared in the past in the literature as "correction" factors for the drag coefficient B. However,

[8] Note that no further poles come from the Debye functions, see (4.31) with (4.28).

these are usually put in by hand and thus seem rather arbitrary — see e.g. the discussion in [34] and references therein. Here, we have derived the general behavior from first principles and see that several terms are necessary to adequately fit the true curves; see eq. (5.1) below. Furthermore, we remark that we expect the divergences at $\beta_T \to 1$ to be resolved by generalizing the theory from linear to non-linear elasticity.

5 Results for Transverse Phonons

In this section we summarize the results of our computations of the drag coefficient in the isotropic approximation for polycrystalline metals whose grains are either face-centered cubic (fcc) or body-centered cubic (bcc). The effective isotropic elastic constants that we use as input data are assembled in Table 1 and were taken from Refs. [17, 35, 36]. Section 2.3 explains how the Lamé and Murnaghan constants are related to the $D_{ijk}^{i'j'k'}$ appearing in our drag coefficient (4.27). The unit cell volumes $V_c = a^3$ (resp. lattice parameters) were taken from Ref. [37, Sec. 12].

	Al (fcc)	Cu (fcc)	Fe (bcc)	Nb (bcc)
a[Å]	4.05	3.61	2.87	3.30
ρ_0[kg/m^3]	2700	8960	7870	8570
λ[GPa]	58.1	105.5	115.5	144.5
μ[GPa]	26.1	48.3	81.6	37.5
$\mathfrak{l}$[GPa]	-143 ± 13	-160 ± 70	-170 ± 40	-610 ± 80
$\mathfrak{m}$[GPa]	-297 ± 6	-620 ± 10	-770 ± 10	-220 ± 30
$\mathfrak{n}$[GPa]	-345 ± 4	-1590 ± 20	-1520 ± 10	-300 ± 20

Table 1: We list the experimental values used in the computation of the drag coefficient: The lattice parameters a and densities ρ_0 were taken from Ref. [37, Sec. 12]. The Lamé constants were taken from Refs. [17], [38, p. 10]. The Murnaghan constants for Cu and Fe were taken from [35], those for Al were taken from Reddy 1976 as reported by Wasserbäch in Ref. [36], and those for Nb were finally taken from [39]. Uncertainties (as given in those references) are listed as well. For the unit cell volume we use $V_c = a^3$, and $b = a/\sqrt{2}$ for fcc metals and $b = a\sqrt{3}/2$ for bcc metals (see Refs. [40] and [11, Sec. 9] for a discussion of Burgers vectors in various crystals).

In particular, we consider the interaction with transverse phonons (i.e. $s = \mathrm{T}$, neglecting $s = \mathrm{L}$ for now), for the metals listed in Table 1, i.e. considering the cutoff-free interaction with transverse phonons within the Debye approximation at room temperature. After performing the integral over ϕ' analytically using (4.22), we solve the remaining three integrals of (4.27) numerically (with Mathematica). The resulting drag coefficients for edge and screw dislocations (using the deformation fields of Section 3) are plotted in Figures 4 and 5.

The predominant sources of uncertainty at the moment are the uncertainties in the elastic constants and not knowing which size and shape to take for the dislocation core cutoff (which can significantly affect the magnitude and shape of the $B(v)$ curve unless it is much smaller than a Burgers vector).

From Figures 4 and 5 we see that the drag coefficient is not very sensitive to the dislocation velocity in the regime where $\beta_T \ll 1$, and as pointed out above the exact shape of the curve (albeit not its general behavior) is somewhat sensitive to the cutoff and the elastic constants. Our

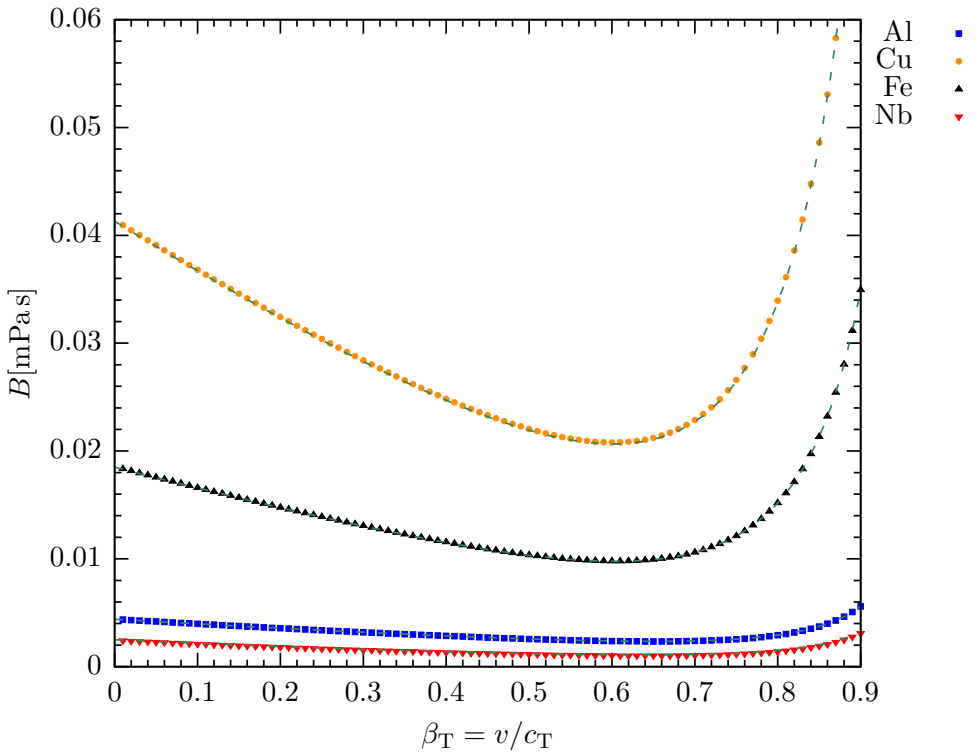

Figure 4: The drag coefficient from phonon wind for edge dislocations in various metals in the Debye approximation with zero dislocation core size (i.e. no cutoff), with isotropic second and third order elastic constants from Table 1. Three integrals (over t, ϕ, q') were done numerically at $T = 300\,\mathrm{K}$ taking into account only the interaction with transverse phonons. Furthermore, the numerical results are overlain with least-squares-fitted curves (dashed lines) of the form given in eq. (5.1) with coefficients from Table 2.

curves start at $\beta_T = 0.01$, i.e. around the speed where the dislocation velocity typically becomes linearly dependent on the applied stress [2], hence the motion can be described as "viscous". (At significantly lower velocities, experiments typically find a power law dependence, $v \propto \sigma^m$.) At higher velocities the drag coefficient increases rapidly with velocity, consistent with experiments done in the velocity regime $0.1 < \beta_T < 0.5$ for LiF crystals [41], but not with other experiments done up to $\beta_T < 0.7$ for NaCl crystals [42] (the latter have exhibited a linear stress-velocity dependence even in this regime).

At around half transverse sound speed, the drag coefficient starts to grow with dislocation velocity. Close to sound speed this growth becomes very steep (at least for edge dislocations), but this might signal the breakdown of the present theory rather than be an actual effect (which is why the figures are displayed only up to 90% sound speed). We will need experimental data and/or MD simulations to determine exactly how close to transverse sound speed the current theory remains valid.

All curves shown in Figures 4 and 5 above can be fitted quite accurately using functions of

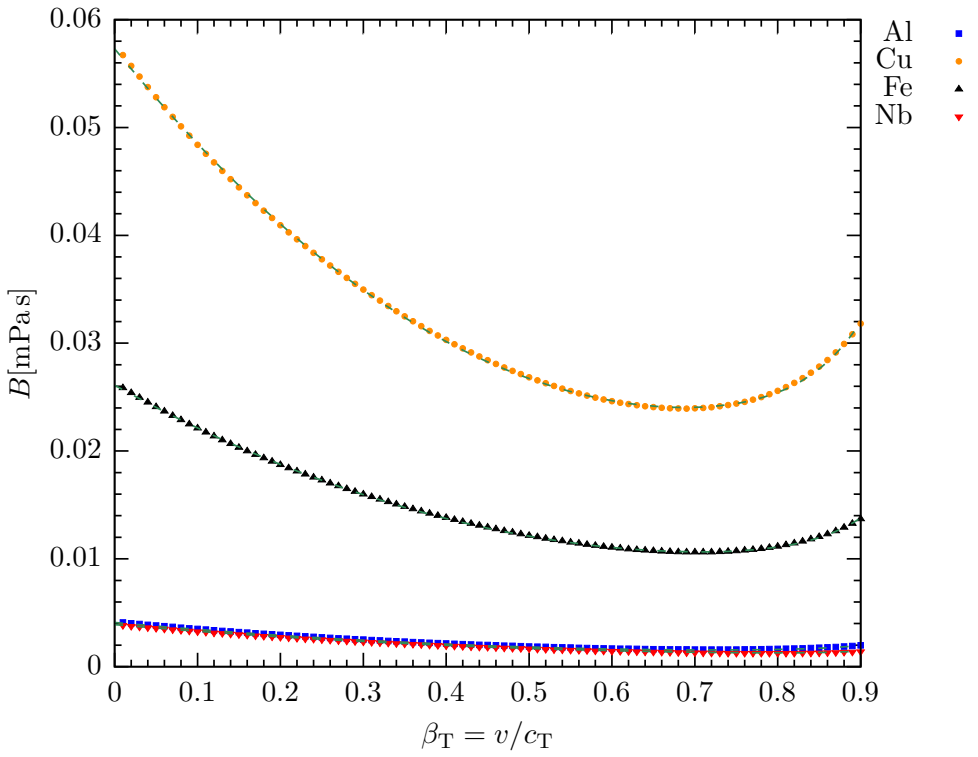

Figure 5: The drag coefficient from phonon wind for screw dislocations in various metals in the Debye approximation with zero dislocation core size (i.e. no cutoff) and with isotropic second- and third-order elastic constants from Table 1. Once more, three integrals (over t, ϕ, q') were done numerically at $T = 300\,\mathrm{K}$ taking into account only the interaction with transverse phonons. Again, the numerical results are overlain with least-squares-fitted curves (dashed lines) of the form given in eq. (5.1) with coefficients from Table 2.

the form

$$\begin{aligned} B_\mathrm{e}(\beta_\mathrm{T}) &\approx C_0^\mathrm{e} + C_1^\mathrm{e}\beta_\mathrm{T} + C_2^\mathrm{e}\beta_\mathrm{T}^2 + C_3^\mathrm{e}\log\left(1-\beta_\mathrm{T}^2\right) + C_4^\mathrm{e}\left(\frac{1}{\sqrt{1-\beta_\mathrm{T}^2}} - 1\right), \\ B_\mathrm{s}(\beta_\mathrm{T}) &\approx C_0^\mathrm{s} + C_1^\mathrm{s}\beta_\mathrm{T} + C_2^\mathrm{s}\beta_\mathrm{T}^2 + C_3^\mathrm{s}\beta_\mathrm{T}^4 + C_4^\mathrm{s}\beta_\mathrm{T}^{16}, \end{aligned} \tag{5.1}$$

for edge (B_e) and screw (B_s) dislocations. The forms of these functions were motivated by the asymptotic behavior as $\beta_\mathrm{T} \to 1$ in accordance with Subsection 4.3 and the discussion in Appendix B together with the next-to-leading-order term in the small-velocity expansion of eq. (5.3) below. Additional polynomial powers in β_T were needed to get good fits at intermediate velocities. Explicit values for the coefficients $C_{0\text{-}3}^{\mathrm{e/s}}$ for edge/screw dislocations for the metals shown above are easily computed using least squares fits[9], and are given in Table 2. The resulting curves are overlain with the numerical data in Figures 4, 5.

Comparing our results (in the low velocity regime without any cutoff, cf. Table 1) to experiments and MD simulations, we note that

- Al (fcc aluminum) is below the range of experimental values of $\sim 0.02\,\mathrm{mPas}$ in [43] and $\sim 0.06\,\mathrm{mPas}$ in [44], and also below MD simulations ($\sim 0.01\,\mathrm{mPas}$ for edge and $\sim 0.02\,\mathrm{mPas}$

[9] The best fit was achieved by using the data up to $85\%c_\mathrm{T}$, and in the edge case fitting the log of the data.

	Al (fcc)	Cu (fcc)	Fe (bcc)	Nb (bcc)
C_0^{e}	0.0044	0.0414	0.0186	0.0024
C_1^{e}	-0.0044	-0.0470	-0.0197	-0.0035
C_2^{e}	0.0025	0.0233	0.0110	0.0030
C_3^{e}	0.0070	0.1032	0.0458	0.0052
C_4^{e}	0.0114	0.1809	0.0783	0.0078
C_0^{s}	0.0041	0.0573	0.0261	0.0039
C_1^{s}	-0.0069	-0.0946	-0.0425	-0.0065
C_2^{s}	0.0047	0.0667	0.0289	0.0043
C_3^{s}	-0.0001	0.0008	0.0004	-0.0005
C_4^{s}	0.0018	0.0285	0.0122	0.0013
B_{e}	0.0044	0.0409	0.0184	0.0024
B_{s}	0.0041	0.0567	0.0259	0.0038

Table 2: Fitting parameters $C_m^{\mathrm{e}}/C_m^{\mathrm{s}}$ for edge/screw dislocations in units of mPas. In the last two lines we report (again in units of mPas) the numerically computed results for the drag coefficient at 1% sound speed, i.e. $\beta_{\mathrm{T}} = 0.01$.

for screw dislocations in [45]),

- Cu (fcc copper) is well within the range of experimental values of $\sim 0.0079\,\mathrm{mPas}$ in [46], $\sim 0.02\,\mathrm{mPas}$ in [47, 48], $\sim 0.065\,\mathrm{mPas}$ (for both edge and screw dislocations) in [49], $\sim 0.07\,\mathrm{mPas}$ in [50], and $\sim 0.08\,\mathrm{mPas}$ in [51],
- Fe (bcc iron) is lower than the experimental values of $\sim 0.34\,\mathrm{mPas}$ for edge and $\sim 0.661\,\mathrm{mPas}$ for screw dislocations reported in [52], as well as the result of MD simulations of $\sim 0.26\,\mathrm{mPas}$ for screw dislocations reported in [53],

Unless we have stated explicitly otherwise, the experimental values we compare to are either of mixed edge/screw type or unknown.

Temperature and pressure dependence

All results above were computed for zero pressure and room temperature, i.e. 300 K, because the elastic constants we used were measured at this temperature; see Table 1. From eq. (4.31) and eq. (4.35) we see that the drag coefficient grows roughly linearly with T at sufficiently high temperatures. In fact, for temperatures above the Debye temperature, the equilibrium phonon distribution functions may be expanded as

$$(n_{q'-q} - n_{q'}) \approx \frac{k_{\mathrm{B}} T \Omega_q}{\hbar \omega_{q'} \omega_{q'-q}} - \frac{\hbar \Omega_q}{12 k_{\mathrm{B}} T} + \mathcal{O}\Big(1/(k_{\mathrm{B}}T)^3\Big) \,, \tag{5.2}$$

even before making use of the linear dispersion relation. Clearly the linear temperature dependence is thus independent of the explicit form of $\omega_{q'}$.

However, with increasing T, the elastic constants will also change; this introduces an additional temperature dependence into the phonon wind contribution to the drag coefficient. Krasnikov et al. [34] claim (based on MD simulations) that the temperature dependence of the drag coefficient B receives a fourth power correction at very high temperatures, i.e. $B(T)/B(\Theta) \sim T/\Theta + 0.077(T/\Theta)^4$ where Θ is the Debye temperature. At this point, however, it is unclear

whether the temperature dependence of the elastic constants can account for this change, and also if the fourth power correction represents the true temperature behavior of the phonon wind. We will investigate the temperature dependence of the drag coefficient further in a future work. For now, we just mention that the shear modulus can be modeled by a *linearly decreasing* function with temperature [1, 54, 55], meaning that those terms which are proportional to μ or μ^2 in the drag coefficient B will *not* grow as T^4, and it is unclear whether the Murnaghan constants will lead to this behavior.

We also postpone the derivation of the pressure dependence of the phonon wind to future work.

Approximation for small velocity and large temperature

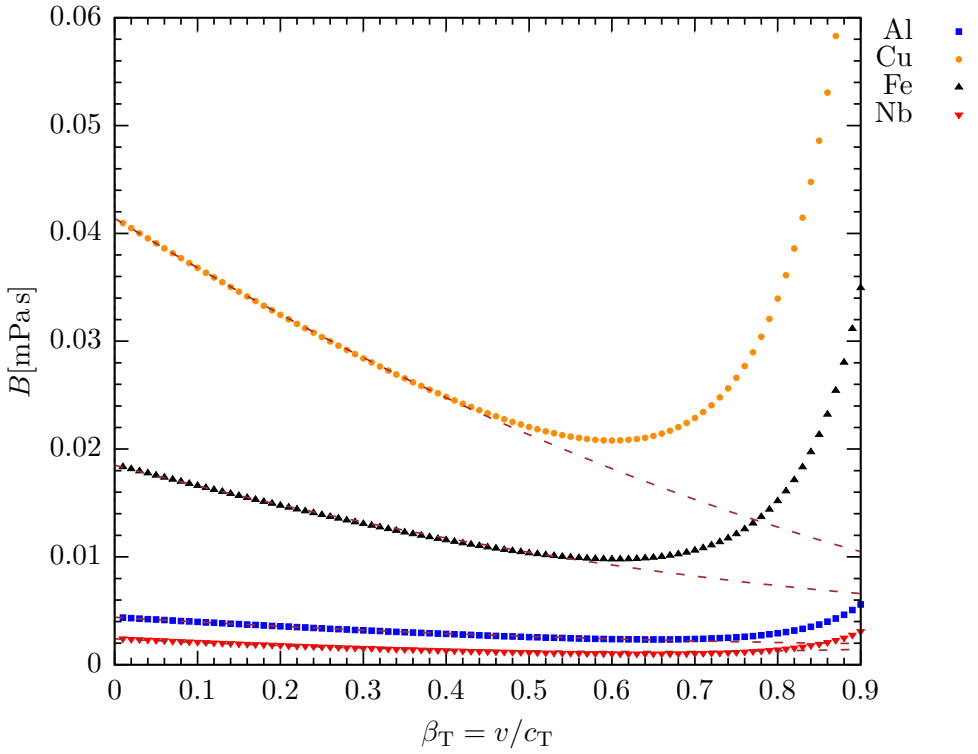

Figure 6: The drag coefficient from phonon wind for edge dislocations in various metals, overlain with the small velocity (large temperature) approximation of eq. (5.3), (5.4).

Let us go back to eq. (4.27) for the drag coefficient in the isotropic approximation. Since most applications involve temperatures around and above the Debye temperature, we use the temperature expansion (4.31) up to next-to-leading order. Upon expanding (up to next-to-leading order) for small dislocation velocities ($\beta_T \ll 1$), we may compute the remaining integrals analytically, and can compare the leading-order term to previous work such as [22]. Additionally, we drop the mixed terms proportional to $\beta_T^2/(k_B T)$, since they are small compared to the others for large T and small β_T. In this case we find for the interaction of edge and screw dislocations

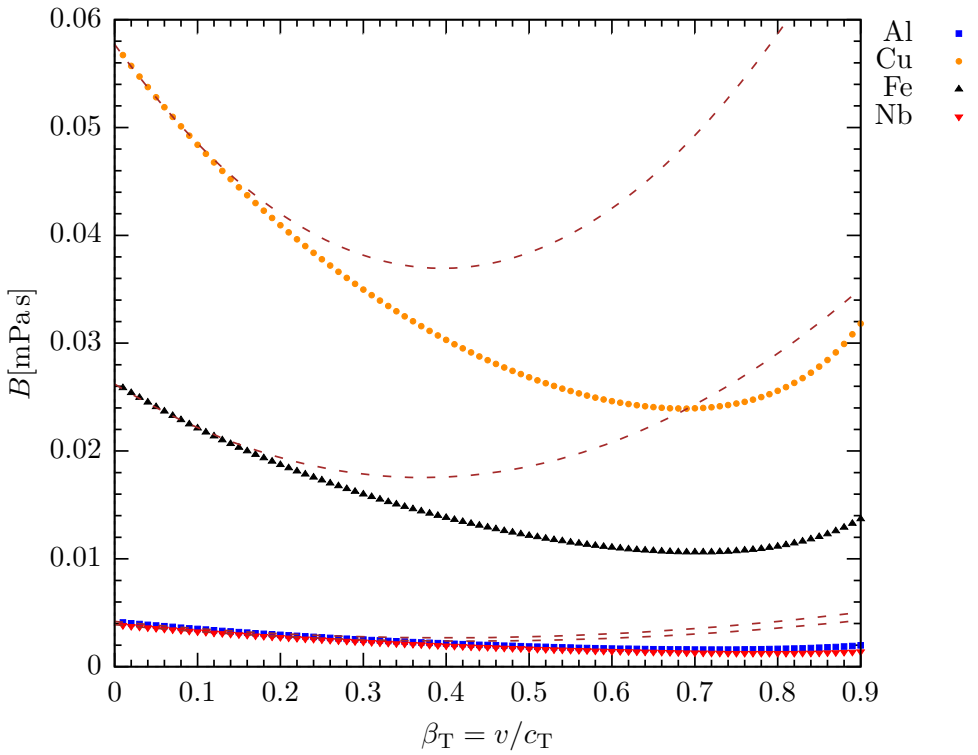

Figure 7: The drag coefficient from phonon wind for screw dislocations in various metals, overlain with the small velocity (large temperature) approximation of eq. (5.3), (5.5).

with transverse phonons (i.e. $s = \mathrm{T}$):

$$B \approx \frac{b^2}{5(8\mu)^2}\left(\left[\frac{k_{\mathrm{B}}T\sqrt[3]{3}\left(\frac{\pi}{2}\right)^{\frac{2}{3}}}{c_{\mathrm{T}}V_{\mathrm{c}}^{\frac{4}{3}}} - \frac{\pi^2 c_{\mathrm{T}}\hbar^2}{6k_{\mathrm{B}}TV_{\mathrm{c}}^2}\right] f_0(\lambda,\mu,\mathfrak{m},\mathfrak{n}) \right.$$
$$\left. - \frac{\beta_{\mathrm{T}}}{\pi}\left[\frac{k_{\mathrm{B}}T\sqrt[3]{2}\left(\frac{\pi}{3}\right)^{\frac{2}{3}}}{c_{\mathrm{T}}V_{\mathrm{c}}^{\frac{4}{3}}} - \frac{\pi^2 c_{\mathrm{T}}\hbar^2}{6k_{\mathrm{B}}TV_{\mathrm{c}}^2}\right] f_1(\lambda,\mu,\mathfrak{m},\mathfrak{n}) + \beta_{\mathrm{T}}^2 \frac{k_{\mathrm{B}}T\left(\frac{9\pi}{16}\right)^{\frac{2}{3}}}{7c_{\mathrm{T}}V_{\mathrm{c}}^{\frac{4}{3}}} f_2(\lambda,\mu,\mathfrak{m},\mathfrak{n})\right), \quad (5.3)$$

where the coefficients $f_{0,1,2}$ depend only on the elastic constants λ, μ, $\mathfrak{m}$, $\mathfrak{n}$ (not $\mathfrak{l}$), and their explicit form depends on whether we consider edge or screw dislocations. In particular, for edge dislocations the coefficients read

$$f_0^{\mathrm{e}}(\lambda,\mu,\mathfrak{m},\mathfrak{n}) = \Big[516(2\mu)^4 + 165\lambda^2\mathfrak{n}^2 + 16\mu^2(370\lambda^2 + 151\mathfrak{m}^2 + 274\lambda\mathfrak{m} - 44\mathfrak{m}\mathfrak{n} + 15\mathfrak{n}^2 + 119\lambda\mathfrak{n})$$
$$+ 96\mu^3(133\lambda + 64\mathfrak{m} + 4\mathfrak{n}) + 2\lambda\mu\mathfrak{n}(764\lambda + 76\mathfrak{m} + 141\mathfrak{n})\Big]/\left[84(\lambda+2\mu)^2\right],$$
$$f_1^{\mathrm{e}}(\lambda,\mu,\mathfrak{m},\mathfrak{n}) = \Big[2\mu^2\left(798\lambda^2 + 6(8\mathfrak{m})^2 + 8\mathfrak{m}(42\lambda - 19\mathfrak{n}) + 51\mathfrak{n}^2 + 296\lambda\mathfrak{n}\right) + 183(2\mu)^4 + \frac{111\lambda^2\mathfrak{n}^2}{2}$$
$$+ 16\mu^3(235\lambda + 92\mathfrak{m} + 11\mathfrak{n}) + 2\lambda\mu\mathfrak{n}(206\lambda - 36\mathfrak{m} + 61\mathfrak{n})\Big]/\left[5(\lambda+2\mu)^2\right],$$

$$
\begin{aligned}
f_2^{\mathrm{e}}(\lambda,\mu,\mathfrak{m},\mathfrak{n}) = \Big[&4\mu^3\left(6933(4\lambda)^2+2952(4\mathfrak{m})^2+520\lambda(102\mathfrak{m}-7\mathfrak{n})-22076\mathfrak{m}\mathfrak{n}+3977\mathfrak{n}^2\right)\\
&+2\lambda\mu^2\left(1969(4\lambda)^2+8486(2\mathfrak{m})^2+4\mathfrak{m}(1676\lambda-8673\mathfrak{n})+9951\mathfrak{n}^2+6708\lambda\mathfrak{n}\right)\\
&+4\lambda^2\mu\mathfrak{n}(2661\mathfrak{n}-38\lambda-4540\mathfrak{m})+96\mu^4(9021\lambda+3260\mathfrak{m}-259\mathfrak{n})\\
&+18814(2\mu)^5+1411\lambda^3\mathfrak{n}^2\Big]/\left[198(\lambda+2\mu)^3\right],
\end{aligned}
\tag{5.4}
$$

whereas for screw dislocations they compute to

$$
\begin{aligned}
f_0^{\mathrm{s}}(\lambda,\mu,\mathfrak{m},\mathfrak{n}) &= \frac{1}{7}\left(33(2\mu)^2+62\mu\mathfrak{n}+\frac{131}{12}\mathfrak{n}^2\right),\\
f_1^{\mathrm{s}}(\lambda,\mu,\mathfrak{m},\mathfrak{n}) &= 41(2\mu)^2+76\mu\mathfrak{n}+\frac{27}{2}\mathfrak{n}^2,\\
f_2^{\mathrm{s}}(\lambda,\mu,\mathfrak{m},\mathfrak{n}) &= \frac{1}{11}\left(\frac{3635(2\mu)^2}{3}+2202\mu\mathfrak{n}+\frac{1457\mathfrak{n}^2}{4}\right).
\end{aligned}
\tag{5.5}
$$

The simpler structure in the screw case is partly due to the deformation field depending only on c_{T}, whereas the deformation field for edge dislocations also includes terms depending on c_{L}; see (3.10), (3.12). In fact, in order to arrive at (5.4) we used the relation $c_{\mathrm{L}} = c_{\mathrm{T}}\sqrt{\frac{\lambda+2\mu}{\mu}}$, cf. (4.23). Additionally, the coefficients in the screw case depend only on μ and $\mathfrak{n}$. Notice that the first term in (5.3) qualitatively agrees with [10] Ref. [22], albeit differing in some numerical coefficients within $f_0^{\mathrm{e,s}}$. This discrepancy can be traced back to the tensor of third order elastic constants used in that paper which seems to be incorrect.

Plugging in the experimental data of Table 1, we may compare with our numerical results. Figures 6, 7 show good agreement of (5.3) below 40%–50% transverse sound speed (depending on the metal). Finally, Table 3 lists the (dimensionless) values of the coefficients $f_{0,1,2}^{\mathrm{e,s}}/(8\mu)^2$ for various metals.

	Al (fcc)	Cu (fcc)	Fe (bcc)	Nb (bcc)
$f_0^{\mathrm{e}}/(8\mu)^2$	2.877	15.88	4.353	0.468
$f_1^{\mathrm{e}}/(8\mu)^2$	14.29	86.72	22.84	3.392
$f_2^{\mathrm{e}}/(8\mu)^2$	12.62	50.85	14.84	5.045
$f_0^{\mathrm{s}}/(8\mu)^2$	2.723	22.15	6.172	0.747
$f_1^{\mathrm{s}}/(8\mu)^2$	23.72	192.1	53.63	6.562
$f_2^{\mathrm{s}}/(8\mu)^2$	55.94	464.6	128.1	14.98

Table 3: List of coefficients derived from second- and third-order elastic constants for various metals, as they appear in the small velocity expansion of the drag coefficient, eq. (5.3). All values in this list are dimensionless.

6 Conclusion and Outlook

In this paper we have studied the velocity dependence of the dislocation drag coefficient for dislocation velocities v in the range $0.01c_{\mathrm{T}} < v < c_{\mathrm{T}}$ where c_{T} is the transverse sound speed.

[10] Though here, we removed the cutoff for the dislocation core and expanded for large temperature. Furthermore, in order to compare the two expressions we note that the wave vector cutoff denoted in [25] by k_{D} is related to the unit cell volume, $k_{\mathrm{D}} \propto V_{\mathrm{c}}^{-1/3}$.

In this regime the dominant contribution to dislocation drag is the dissipative interaction with phonons, i.e. the phonon wind. Although the currently employed model breaks down at $v = c_{\mathrm{T}}$, we were able to make predictions for the velocity dependence of the drag coefficient $B(v)$ at dislocation speeds below this critical value. Our main results are captured in Figures 4 and 5 for edge and screw dislocations respectively, for eight different metals chosen for their simple lattice structure and available data for their third-order elastic constants at room temperature. We computed $B(v)$ in the range $v/c_{\mathrm{T}} \in [0.01, 0.08]$ and can represent all results by simple fitting functions of the form eq. (5.1) with four fitting parameters. Surprisingly — considering the highly non-trivial dependence on v — the drag coefficient turns out to be nearly constant below 40% transverse sound speed for most of the metals considered here. Furthermore, we have compared our results to experimental values and MD simulation results where these are available, i.e. in the low-velocity regime, i.e. $v/c_{\mathrm{T}} \sim 0.01$. We found good agreement for copper, while our results for aluminum and iron are lower in the low-velocity regime. Additional experimental data on third-order elastic constants is necessary to improve our predictions and to compute the drag coefficient for other materials.

Our future work will include calculating

- the temperature and density dependence of B,
- the drag coefficient for near-sonic and possibly supersonic dislocation speeds,
- and $B(v)$ for more complicated lattice structures. The latter will necessitate deviations from isotropy, the inclusion of optical phonons and hence more sophisticated dispersion relations to capture the impact of the phonon spectra on the drag coefficient.

Acknowledgements

We thank Darby J. Luscher and Benjamin A. Szajewski for enlightening discussions. This work was performed under the auspices of the U.S. Department of Energy under contract DE-AC52-06NA25396. In particular, the authors are grateful for the support of the Advanced Simulation and Computing, Physics and Engineering Models Program.

A Fourier Transform of Displacement Gradients and Cutoffs

Dislocations have finite core sizes r_0 and in a dense ensemble of dislocations the strain fields are screened away at distances of order the mean distance between dislocations α. Hence, these parameters could be used to cut off the Fourier integrals: Defining

$$\hat{d}_{i,j}(q, \phi, r_0, \alpha) = \int_{r_0}^{\alpha} dr r \int_0^{2\pi} d\theta d_{i,j}(r, \theta) e^{-iqr\cos(\theta-\phi)}\,, \tag{A.1}$$

we get (for $\beta_{\mathrm{T,L}} \to 0$) the following general type of integral

$$\begin{aligned}\int_{r_0}^{\alpha} dr \int_0^{2\pi} \frac{d\theta}{\pi} (A\sin\theta + B\cos\theta) e^{-iqr\cos(\theta-\phi)} &= -\frac{2i}{q}\Big[A\sin\phi + B\cos\phi\Big] \int_{qr_0}^{q\alpha} dx\, J_1(x) \\ &= -\frac{2i}{q}\Big[A\sin\phi + B\cos\phi\Big]\,(J_0(qr_0) - J_0(q\alpha))\end{aligned} \tag{A.2}$$

where $J_n(x)$ denotes the Bessel function of the first kind [56]. In the limit $\alpha \to \infty$ and $r_0 \to 0$ we have $(J_0(qr_0) - J_0(q\alpha)) \to 1$. It then follows that

$$\int_0^\infty dr \int_0^{2\pi} \frac{d\theta}{\pi} (A\sin\theta + B\cos\theta) e^{-iqr\cos(\theta-\phi)} = \frac{-2i}{q}\Big[A\sin\phi + B\cos\phi\Big], \tag{A.3}$$

or in Cartesian coordinates

$$\int_{-\infty}^\infty \int_{-\infty}^\infty \frac{dxdy}{\pi} \frac{(Ay+Bx)}{x^2+y^2} e^{-i(xq_x+yq_y)} = \frac{-2i}{q_x^2+q_y^2}\Big[Aq_y + Bq_x\Big]. \tag{A.4}$$

From these results we may deduce the Fourier transform of the expressions with non-vanishing β, namely

$$\int_{-\infty}^\infty \int_{-\infty}^\infty \frac{dxdy}{\pi} \frac{(Ay+Bx)}{x^2+\gamma^{-2}y^2} e^{-i(xq_x+yq_y)} = \frac{-2i}{\gamma^{-2}q_x^2+q_y^2}\left[A\gamma q_y + \frac{Bq_x}{\gamma}\right] = \frac{-2i\left[A\gamma^2\sin\phi + B\cos\phi\right]}{q\gamma\left(1-\beta^2\cos^2\phi\right)}, \tag{A.5}$$

where we simply rescaled y and q_y to arrive at the same type of integral as before. Note, that this trick fails if we keep the cutoffs in which case the integral over θ cannot easily be done. Nonetheless, in the limits of infinitesimal dislocation core size and infinite separation between dislocations we arrive at (3.10) for edge dislocations and at (3.12) for screw dislocations. Taking the limits $r_0 \to 0$ and $\alpha \to \infty$ greatly simplified the expressions, and we will investigate below how good an approximation this is. In any case, since all expressions converge, the cutoffs are not necessary from a mathematical point of view.

On the effect of cutoffs

The rescaling trick used for (A.5) above entailed an integral $\int dR$ where $R^2 = x^2 + \gamma^{-2}y^2$. Thus, in changing the size of the cutoffs in the y direction to match the current symmetry leads to $\int_{\tilde{r}_0}^{\tilde{\alpha}} dR$ where $\tilde{r}_0 = r_0\sqrt{1-\beta^2\sin^2\theta}$ and likewise $\tilde{\alpha} = \alpha\sqrt{1-\beta^2\sin^2\theta}$. The result for the Fourier transform is then to be multiplied by

$$\left(J_0(q\tilde{r}_0\sqrt{1-\beta^2\cos^2\phi}) - J_0(q\tilde{\alpha}\sqrt{1-\beta^2\cos^2\phi})\right),$$

which in the limit $\tilde{r}_0 \to 0$, $\tilde{\alpha} \to \infty$ tends to 1. Note that all factors of β appearing here are either β_L or β_T depending on which of the two appeared next to y before Fourier transforming, i.e. this simple result follows from choosing two different cutoffs (with β_T or β_L) for different terms in the deformation field. For small velocities, however, the effect of this further simplification is small.

On the other hand, since we are merely interested in a rough estimate of the magnitude of possible corrections depending on the magnitudes of r_0 and α, the approximations above are sufficient. q will be integrated from 0 to q_BZ, so taking the mean value of $q_\mathrm{BZ}/2$ and neglecting the velocity dependence ($\beta \to 0$), we have $(J_0(q_\mathrm{BZ}r_0/2) - J_0(q_\mathrm{BZ}\alpha/2))$. Let us write both cutoffs

in units of Burgers vectors, $\hat{r}_0 = r_0/b$, $\hat{\alpha} = \alpha/b$. Then our Bessel functions read

$$\left(J_0(A\sqrt[3]{6\pi^2}\hat{r}_0/4) - J_0(A\sqrt[3]{6\pi^2}\hat{\alpha}/4)\right) \approx \left(1 - \frac{(0.97A\hat{r}_0)^2}{4} + \mathcal{O}(\hat{r}_0^4)\right) - \left(\sqrt{\frac{2}{(0.97A\pi\hat{\alpha})}}\cos\left(0.97A\hat{\alpha} + \pi/4\right) + \mathcal{O}(1/\hat{\alpha})\right)$$

where $A = \sqrt{2}$ for fcc metals and $A = \sqrt{3}$ for bcc metals. This expression leads to corrections from either cutoff of the order of (or less than) 10% for $r_0 < b/3$ and $\alpha > 50b$. In fact, some references (e.g. [11, 57]) argue that the cutoff r_0 should be of the order of 30% of a Burgers vector. Furthermore, α of the order of 50 Burgers vectors or less would correspond to very high dislocation densities. Thus, for most cases we do not expect a significant impact on the result for the drag coefficient from phonon wind by taking the limits $r_0 \to 0$ and $\alpha \to \infty$. However, as the dislocation velocity approaches the transverse sound speed, this assessment will no longer be true — see our discussion in Section 3. Therefore, we intend to study more thoroughly the effect of the dislocation core on the drag coefficient in future work.

B Drag Coefficients for Transverse Phonons as $v \to c_{\mathbf{T}}$

B.1 Screw Dislocations Interacting with Transverse Phonons

The drag coefficient may be written

$$B = \frac{D}{v^2} = \frac{4\pi}{\hbar v^2}\int\frac{d^3\mathbf{k}}{(2\pi)^3}\int\frac{d^3\mathbf{k}'}{(2\pi)^3}\int\frac{d^2\mathbf{q}}{(2\pi)^2}\,(2\pi)^3\,\delta^3(\mathbf{k}'-\mathbf{k}-\mathbf{q})\times \times\sum_{ss'}\delta(\omega_{s'}(k') - \omega_s(k) - \mathbf{q}\cdot\mathbf{v})(\mathbf{q}\cdot\mathbf{v})\left[n(\omega_s(k)) - n(\omega_{s'}(k'))\right]\left|\Gamma_{ss'}(\mathbf{k},\mathbf{k}')\right|^2 \tag{B.1}$$

where $\mathbf{k} = \mathbf{q}''$ and $\mathbf{k}' = \mathbf{q}'$ are the momenta of the incoming and scattered phonon respectively and $\mathbf{q} = \mathbf{k}' - \mathbf{k}$ is the Fourier transform variable of the dislocation, $\mathbf{v}$ is its velocity, $\omega_s(k)$ is the energy of a phonon with polarization s, $n(\omega(k))$ is the thermal equilibrium Bose-Einstein distribution function for that energy, and $\Gamma_{ss'}$ is a direction-dependent matrix element squared of the third order Hamiltonian vertex, given by (4.9), with s, s' labeling the initial and final phonon polarization states (transverse T or longitudinal L), respectively.

We choose to use Cartesian coordinates here because the velocity of the dislocation $\mathbf{v}$ selects a direction, i.e. the $\hat{x}$ direction. Since the infinitely extended dislocations are assumed independent of z, we also have $q_z = 0$ and hence $k'_z = k_z$. Second, we take one kind of dislocation (edge or screw) at a time, and one pair of phonon polarizations TT, LL, or TL at a time in order to analyze the limit $v \to c_{\mathrm{T}}, c_{\mathrm{L}}$ separately, where the Fourier transforms of the dislocation profiles become singular. For the sake of brevity, we discuss in detail only the simplest case of screw dislocations interaction with transverse phonons (which dominate over the longitudinal ones). Third, we put aside the polarization term involving the $\Gamma_{ss'}$ at first, and just look at the degree of divergence/convergence of the remaining integrals as $v \to c$, and after that examine the effect of the vertex part for various cases of polarizations and kind of dislocation.

In the Cartesian coordinates just described, we perform the $\mathbf{k}'$ integral first by using the δ-function, so that

$$k'_z = k_z \qquad k'_x = k_x + q_x \qquad k'_y = k_y + q_y \tag{B.2}$$

and then perform the k_z integral by using the final δ function of energy conservation. Also, we restrict our present calculation to the case where both polarizations are either transverse or longitudinal, but not mixed. In this case, we may replace $\omega_{s'} \to \omega_s$ under the sum, and to avoid notational clutter we drop the polarization subscripts from the phonon energies for the remainder of this appendix. In this way (B.1) reduces to

$$B = \frac{2}{\hbar v} \sum_{ss'} \int \frac{d^2\mathbf{k}_\perp}{(2\pi)^2} \int \frac{d^2\mathbf{q}}{(2\pi)^2}\; q_x \left|\frac{\partial \Delta E}{\partial k_z}\right|^{-1} \left[n(\omega(k)) - n(\omega(k'))\right] \left|\Gamma_{ss'}(\mathbf{k},\mathbf{k}')\right|^2_{\mathcal{C}} \tag{B.3}$$

which are now two two-dimensional integrals in the (x, y) plane perpendicular to the $\hat{z}$ axis. In (B.3) the condition $\mathcal{C}$ is shorthand for the condition (B.2) on the components of $\mathbf{k}'$ which should be solved for and substituted, together with the energy conservation condition

$$\Delta E \equiv \omega(k') - \omega(k) - q_x v = 0 \tag{B.4}$$

to be set to zero after evaluating the Jacobian factor $\left|\frac{\partial \Delta E}{\partial k_z}\right|^{-1}$ in (B.3). To evaluate that Jacobian, we use the simple linear phonon dispersion relation

$$\omega(k) = c|\mathbf{k}| = ck = c\sqrt{k_x^2 + k_y^2 + k_z^2} \tag{B.5}$$

for the phonons (with $c = c_{\rm T}$ or $c = c_{\rm L}$ for transverse or longitudinal phonons respectively), and

$$\frac{\partial \Delta E}{\partial k_z} = \frac{c^2 k_z}{\omega(k')} - \frac{c^2 k_z}{\omega(k)} = -\frac{c^2 q_x\, v\, k_z}{\omega(k')\omega(k)} \tag{B.6}$$

after the condition $\Delta E = 0$ is used. Thus we obtain

$$B = \frac{2}{\hbar v^2} \sum_{ss'} \int \frac{d^2\mathbf{k}_\perp}{(2\pi)^2} \int \frac{d^2\mathbf{q}}{(2\pi)^2}\; \frac{q_x}{|q_x|}\, \frac{\omega(k)\omega(k')}{c^2|k_z|} \left[n(\omega(k)) - n(\omega(k'))\right] \left|\Gamma_{ss'}(\mathbf{k},\mathbf{k}')\right|^2_{\mathcal{C}}. \tag{B.7}$$

In examining potential divergences the first key point is to analyze the $|k_z|$ denominator in (B.7), where we recall that k_z must be solved for by using the condition $\Delta E = 0$. Using also the linear phonon dispersion relation (B.5) we obtain after some algebra

$$k_z(\mathbf{k}_\perp, \mathbf{q}) = \pm \frac{1}{2q_x\beta} \sqrt{\left[q_x^2\,(1-\beta^2) + q_y^2 + 2\mathbf{k}_\perp \cdot \mathbf{q}\right]^2 - 4q_x^2\,\beta^2\,\mathbf{k}_\perp^2} \tag{B.8}$$

with $\beta = v/c$. Note that (B.8) has solutions for real k_z if and only if the argument of the square root is non-negative, which constitutes the main constraint we have to deal with and particularly if $|k_z|$ can approach zero, which may lead to a divergence in (B.7).

Now also observe that the large momentum end of the integrals in (B.7) will be cut off in one of two ways. For low temperatures $k_{\rm B}T \ll \hbar c q_{\rm BZ}$ the thermal distribution function will fall exponentially and the momentum integrals will therefore be cut off by T. On the other hand, for high temperatures $k_{\rm B}T \gg \hbar c q_{\rm BZ}$, the Bose-Einstein thermal distribution can be replaced by its small ω limit, *i.e.*

$$n(\omega) = \frac{1}{\exp\left(\hbar\omega/k_{\rm B}T\right) - 1} \to \frac{k_{\rm B}T}{\hbar\omega} \qquad \text{for} \quad \omega < c q_{\rm BZ} \ll k_{\rm B}T/\hbar \tag{B.9}$$

in which case the momentum integrals will be cut off by $q_{\rm BZ}$ at the edge of the Brillouin zone. Since it is in this latter limit that the short distance singularities of the dislocation are probed

by high velocity motion of the dislocation approaching the speed of sound, we will examine this high temperature limit most closely and use the approximation (B.9). One should then go back at the end to be sure that this presumption is actually correct.

The first case we looked at carefully was that of screw dislocations and transverse phonons, since this is the case that was the most sensitive to the $v \to c$ limit with $c = c_{\rm T}$ here, based on the Fourier transforms for the moving screw dislocation given in (3.12). For the screw dislocation the $\tilde{d}_{zx}$ component is dominant because the only other non-zero component $\tilde{d}_{zy}$ in (3.12) contains a factor of $\gamma_t^{-2} = 1 - (v/c_{\rm T})^2$ which is squared again in B and goes to zero as $v \to c_{\rm T}$. Note that the angular dependence in (3.12) does indicate a more severe collinear divergence at $\phi = 0$ for $\tilde{d}_{zy}$ *vs.* $\tilde{d}_{zx}$, so it is not obvious without detailed calculation which is dominant as $v \to c_{\rm T}$, but at least the behavior of the $\tilde{d}_{zy}$ contribution should be indicative. In that case one can extract the most important terms and factors from $|\Gamma_{ss'}|^2$ in (4.9) and (4.19), namely

$$\sum_{ss'} |\Gamma_{ss'}|^2 \propto \frac{\hbar^2}{\rho_0^2 \omega(k)\omega(k')} |\tilde{d}_{zx}(\mathbf{q})|^2 \times (\text{polynomial in } \mathbf{k}, \mathbf{k}') \,. \tag{B.10}$$

Then using the expression (3.12) expressed in Cartesian coordinates, namely

$$|\tilde{d}_{zx}(\mathbf{q})|^2 = \frac{b^2 \, q_y^2}{\left[q_x^2(1-\beta^2) + q_y^2\right]^2} \tag{B.11}$$

the high temperature approximation (B.9) and (B.10), and the energy conservation condition (B.4) again, inserting these all into (B.7), we arrive at a multiple integral of the form

$$B_{\rm screw,\,tr} \simeq \frac{2b^2 k_{\rm B} T}{(2\pi)^4 \rho_0^2 \beta c_{\rm T}^5} \int dk_x \int dk_y \int dq_x \int dq_y \, \frac{|q_x|}{|\mathbf{k}||\mathbf{k}'||k_z|} \frac{q_y^2}{\left[q_x^2(1-\beta^2) + q_y^2\right]^2} \, \mathcal{P}(\mathbf{k},\mathbf{q})\Big|_{\mathcal{C}} \tag{B.12}$$

for the drag coefficient of screw dislocations due to transverse phonon wind in the high temperature limit. Here $\mathcal{P}$ denotes the polynomial (with positive powers of momenta) that we will have to return to, in the final evaluation, and $\mathcal{C}$ reminds us that everything mist be evaluated on the δ-function conditions used, and with k_z real. This means in particular that

$$\begin{aligned} |\mathbf{k}| &= \sqrt{k_x^2 + k_y^2 + k_z^2} = \frac{|q_x^2(1-\beta^2) + q_y^2 + 2k_x q_y + 2k_y q_y|}{2\beta |q_x|} \,, \\ |\mathbf{k}'| &= \sqrt{(k_x+q_x)^2 + (k_y+q_y)^2 + k_z^2} = |\mathbf{k}| + q_x\beta = \frac{|q_x^2(1+\beta^2) + q_y^2 + 2k_x q_y + 2k_y q_y|}{2\beta |q_x|} \,, \end{aligned} \tag{B.13}$$

after using (B.8). Substituting these expressions and (B.8) into (B.12) gives

$$\begin{aligned} B_{\rm screw,\,tr} \simeq \frac{16 b^2 \beta^2 k_{\rm B} T}{(2\pi)^4 \rho_0^2 c_{\rm T}^5} \int dk_x \int dk_y \int dq_x \int dq_y \, \frac{q_x^4 \, q_y^2}{|(q_x^2 + q_y^2 + 2k_x q_x + 2k_y q_y)^2 - \beta^4 q_x^4|} \times \\ \times \frac{1}{\left[q_x^2(1-\beta^2) + q_y^2\right]^2} \frac{\mathcal{P}(\mathbf{k},\mathbf{q})}{\sqrt{\left[q_x^2\,(1-\beta^2) + q_y^2 + 2k_x q_x + 2k_y q_y\right]^2 - 4q_x^2\,\beta^2\,(k_x^2 + k_y^2)}} \end{aligned} \tag{B.14}$$

where the ranges of the integrals are restricted only by the edges of the first Brillouin zone and the requirement that the argument of the square root is positive.

In this form (B.14) we can now examine the limit of $\beta \to 1$, so that

$$B_{\text{screw, tr}} \to \frac{b^2 k_B T}{\pi^4 \rho_0^2 c_T^5} \int dk_x \int dk_y \int dq_x \int dq_y \, \frac{q_x^4}{q_y^2} \, \frac{1}{|(q_x^2+q_y^2+2k_x q_x+2k_y q_y)^2 - q_x^4|} \times$$
$$\times \frac{\mathcal{P}(\mathbf{k},\mathbf{q})}{\sqrt{\left[q_y^2+2k_x q_x+2k_y q_y\right]^2 - 4q_x^2\,(k_x^2+k_y^2)}} \qquad \text{for} \quad v \to c_T \,. \tag{B.15}$$

Counting the powers of momenta there are 4 powers of q_x in the numerator of this integrand (excluding the polynomial $\mathcal{P}$) and 8 powers of momenta in the denominator. Because of the 4 powers of q_x in the numerator and the cancellation of q_x^4 in the first denominator factor we can be sure that the q_x integral will be dominated by its upper limit of order the Debye momentum q_{BZ}. On the other hand the q_y integral is sensitive to its lower limit because of the $1/q_y^2$ factor. That lower limit is determined by the condition that the argument of the square root (which came from solving for $|k_z|$) must be non-negative. This condition is

$$(q_y^2+2k_y q_y)^2 + 4k_x q_x (q_y^2+2k_y q_y) - 4q_x^2 k_y^2 \geq 0 \tag{B.16}$$

which can be satisfied in either one of two ways:

$$(q_y+k_y)^2 \geq 2|q_x|\sqrt{k_x^2+k_y^2} - 2k_x q_x + k_y^2 \,, \tag{B.17a}$$
$$(q_y+k_y)^2 \leq -2|q_x|\sqrt{k_x^2+k_y^2} - 2k_x q_x + k_y^2 \,. \tag{B.17b}$$

However for $|q_x|$ large and k_y small the latter expression is negative and so the second condition (B.17b) cannot be satisfied. The first condition (B.17a) can be further subdivided into two cases:

$$q_y \geq -k_y + \left[2|q_x|\sqrt{k_x^2+k_y^2} - 2k_x q_x + k_y^2\right]^{\frac{1}{2}} = -k_y + Q \geq 0 \,, \tag{B.18a}$$
$$q_y \leq -k_y - \left[2|q_x|\sqrt{k_x^2+k_y^2} - 2k_x q_x + k_y^2\right]^{\frac{1}{2}} = -k_y - Q \leq 0 \,, \tag{B.18b}$$

where we have defined

$$Q \equiv \left[2|q_x|\sqrt{k_x^2+k_y^2} - 2k_x q_x + k_y^2\right]^{\frac{1}{2}} \geq |k_y| \geq 0 \tag{B.19}$$

from which we see that q_y can only become zero if $k_y = 0$ and $k_x q_x = |k_x q_x|$ is non-negative.

Next we use partial fractions to simplify the first denominator in (B.15) into the form

$$\begin{aligned} &\frac{1}{(q_x^2+q_y^2+2k_x q_x+2k_y q_y)^2 - q_x^4} = \frac{1}{2q_x^2}\left[\frac{1}{q_y^2+2k_y q_y+2k_x q_x} - \frac{1}{q_y^2+2k_y q_y+2k_x q_x+2q_x^2}\right] \\ &\simeq \frac{1}{2q_x^2}\,\frac{1}{q_y^2+2k_y q_y+2k_x q_x} = \frac{1}{2q_x^2}\,\frac{1}{(q_y+k_y)^2+2k_x q_x - k_y^2} \\ &= \frac{1}{2q_x^2}\,\frac{1}{(q_y+k_y)^2 - Q^2 + 2|q_x|\sqrt{k_x^2+k_y^2}} \end{aligned} \tag{B.20}$$

where we can ignore the second term in square brackets in the limit that q_x^2 is large, and the last expression is clearly non-negative by the condition (B.17a). Hence using the results of these

analyses and changing integration variables from q_y to $q' \equiv q_y + k_y$ we can rewrite (B.15) in the form

$$B_{\text{screw, tr}} \to \frac{b^2 k_{\rm B} T}{2\pi^4 \rho_0^2 c_{\rm T}^5} \int dk_x \int dk_y \int dq_x \left[\int_Q^\infty dq' + \int_{-\infty}^{-Q} dq'\right] \frac{q_x^2}{(q'-k_y)^2} \times$$
$$\times \frac{\mathcal{P}(\mathbf{k},\mathbf{q})}{\sqrt{q'^2 - Q^2}} \left[\frac{1}{q'^2 - Q^2 + 2|q_x|\sqrt{k_x^2+k_y^2}}\right] \frac{1}{\sqrt{q'^2 - Q^2 + 4|q_x|\sqrt{k_x^2+k_y^2}}}. \tag{B.21}$$

where we can extend the q' integral to $\pm\infty$ since it is dominated by its smallest absolute values.

It is still not possible to perform this integral in closed form. However if we continue to assume that $|q_x|$ is of order $q_{\rm BZ}$ and much larger than k_y or q_y which are dominated by their lower limits, then we can approximate the last two factors in (B.21) by

$$\left[\frac{1}{q'^2 - Q^2 + 2|q_x|\sqrt{k_x^2+k_y^2}}\right] \frac{1}{\sqrt{q'^2 - Q^2 + 4|q_x|\sqrt{k_x^2+k_y^2}}} \simeq \frac{1}{4|q_x|^{\frac{3}{2}}\,(k_x^2+k_y^2)^{\frac{3}{4}}} \tag{B.22}$$

and the remaining q' integral (ignoring the polynomial $\mathcal{P}$)

$$\int_Q^\infty \frac{dq'}{(q'-k_y)^2} \frac{1}{\sqrt{q'^2-Q^2}} + \int_{-\infty}^{-Q} \frac{dq'}{(q'-k_y)^2} \frac{1}{\sqrt{q'^2-Q^2}}$$
$$= \frac{\partial}{\partial k}\left[\int_Q^\infty \frac{dq'}{(q'-k)} \frac{1}{\sqrt{q'^2-Q^2}} - \int_Q^\infty \frac{dq'}{(q'+k)} \frac{1}{\sqrt{q'^2-Q^2}}\right]_{k=k_y} \tag{B.23}$$

can be performed (where we have replaced $q' \to -q'$ in the second integral). Since

$$\int_Q^\infty \frac{dq'}{(q' \mp k)} \frac{1}{\sqrt{q'^2-Q^2}} = \frac{1}{\sqrt{Q^2-k^2}}\left[\frac{\pi}{2} \pm \sin^{-1}\left(\frac{k}{Q}\right)\right] \tag{B.24}$$

the $\pi/2$ terms drop out of the difference in (B.23) while the $\sin^{-1}$ terms add, and after performing the indicated differentiation with respect to k, we obtain for (B.23)

$$\frac{2}{Q^2-k_y^2}\left[1 + \frac{k_y}{\sqrt{Q^2-k_y^2}} \sin^{-1}\left(\frac{k_y}{Q}\right)\right]. \tag{B.25}$$

Now again because $|q_x| \gg |k_y|$, we can drop the $\sin^{-1}\left(\frac{k}{Q}\right)$ term compared to unity in the brackets above, and since $Q^2 - k_y^2 = 2|q_x|\sqrt{k_x^2+k_y^2} - 2k_x q_x$ then we are left with a very simple multiple integral from (B.21), namely

$$\frac{b^2 k_{\rm B} T}{8\pi^4 \rho_0^2 c_{\rm T}^5} \int dk_x \int dk_y \int dq_x \frac{|q_x|^{\frac{1}{2}}}{(k_x^2+k_y^2)^{\frac{3}{4}}} \left[\frac{1}{|q_x|\sqrt{k_x^2+k_y^2} - k_x q_x}\right] \tag{B.26}$$

still ignoring the polynomial $\mathcal{P}$. Indeed since the last factor in square brackets is

$$\frac{1}{|q_x|\sqrt{k_x^2+k_y^2} - k_x q_x} = \frac{1}{q_x^2 k_y^2}\left[|q_x|\sqrt{k_x^2+k_y^2} + k_x q_x\right] \tag{B.27}$$

and the second term is odd under change of sign of k_x, it vanishes in the $\int dk_x$ integral and (B.26) becomes simply

$$\frac{b^2 k_{\rm B} T}{8\pi^4 \rho_0^2 c_{\rm T}^5} \int \frac{dk_y}{k_y^2} \int \frac{dq_x}{|q_x|^{\frac{1}{2}}} \int \frac{dk_x}{(k_x^2+k_y^2)^{\frac{1}{4}}} \simeq \frac{2b^2 k_{\rm B} T}{\pi^4 \rho_0^2 c_{\rm T}^5} q_{\rm BZ} \int \frac{dk_y}{k_y^2} \tag{B.28}$$

since the q_x and k_x integrals are both dominated by their upper cutoffs at the edge of the Brillouin zone $q_{\rm BZ}$ and

$$\int_{-q_{\rm BZ}}^{q_{\rm BZ}} \frac{dk_x}{(k_x^2+k_y^2)^{\frac{1}{4}}} \simeq \int_{-q_{\rm BZ}}^{q_{\rm BZ}} \frac{dk_x}{|k_x|^{\frac{1}{2}}} = \int_{-q_{\rm BZ}}^{q_{\rm BZ}} \frac{dq_x}{|q_x|^{\frac{1}{2}}} = 4\sqrt{q_{\rm BZ}} \tag{B.29}$$

which justifies *a posteriori* the assumption we have been using that the q_x (and k_x) integrals are dominated by the upper limit $q_{\rm BZ}$ of their range.

We have thus obtained (B.28) which is proportional to $q_{\rm BZ}$ for dislocations traveling at the transverse sound speed $v = c_{\rm T}$ but is linearly infrared divergent in its final k_y integral, if the polynomial $\mathcal{P}$ is ignored, which we assumed at first to understand the structure of the momentum integrations and their important ranges. Of course it is not correct to ignore $\mathcal{P}$ in the expression (B.21) or its antecedents for the drag coefficient due to the phonon wind. As long as there are at least two powers of k_y, q_y or k_z in every term of this polynomial, the infrared divergence in (B.28) will be eliminated, and *all* components of the momentum integrals will be driven to their upper cutoff values of order $q_{\rm BZ}$. Since the polynomial is fourth order in the momenta, we therefore expect no infrared divergence and

$$B \propto f(\mu, \mathfrak{n}) \frac{b^2 k_{\rm B} T q_{\rm BZ}^4}{\rho_0^2 c_{\rm T}^5} \tag{B.30}$$

for the drag coefficient due to transverse phonons of a screw dislocation moving at sound speed. This also means that some of the approximations made in arriving at (B.28) will not be valid, but as long as we are sure that there is no divergence as $v \to c_{\rm T}$, we can return to the original exact expressions and evaluate the finite answer numerically with no approximations. The proportionality factor $f(\mu, \mathfrak{n})$ in eq. (B.30) still depends quadratically on the elastic constants, and observing that $\rho_0^2 c_{\rm T}^4 = \mu^2$ we may scale them out in the expression above, i.e. $f(\mu, \mathfrak{n})/\rho_0^2 c_{\rm T}^5 = f(\mathfrak{n}/\mu)/c_{\rm T}$.

The direction-dependent polynomial for screw dislocations scattering transverse phonons

Using the representation (2.29) of Sec. 2.3 we see that $u_{i,i} = \tilde{d}_{i,i} = 0$ for a screw dislocation and likewise $u_{i,i} = 0$ for transverse phonons so that the first three terms of (2.29) do not contribute to the matrix element of the drag coefficient of a screw dislocation coupled to transverse phonons. It appears that the remaining two terms in (2.29) which involve both the c and h elastic constants should contribute to the drag coefficient for screw dislocations and transverse phonons. We concentrate only on the c term or $\tilde{c}$ term in (2.31) because the h term was not previously considered and there is no available data for this elastic constant. So let us concentrate on the c term also here to construct the polynomial $\mathcal{P}$. Again this is just to analyze possible divergences or their elimination whereas of course all non-zero contributions must be taken account of in the end.

Taking one of the $u_{i,j}$ to be the dislocation field and the other two phonon fields (also denoted by $u_{i,j}$) we have the trilinear interaction

$$\begin{aligned}\mathcal{U}_3\big|_{c\,\text{terms}} &= \frac{3c}{4}\int d^3\mathbf{x}\; d_{ij}\;(u_{j,l}+u_{l,j})\;(u_{i,l}+u_{l,i}) \\ &= \frac{1}{2!}\sum_{i_1 i_2 i_3}\sum_{j_1 j_2 j_3} D^{j_1\,j_2\,j_3}_{i_1\,i_2\,i_3}\Big|_{c\ \text{terms}}\int d^3\mathbf{x}\, u_{i_1,j_1}\, u_{i_2,j_2}\, d_{i_3 j_3}\end{aligned} \tag{B.31}$$

from the c terms in (2.29). Thus the direction dependent tensorial coefficient is

$$D^{j_1\,j_2\,j_3}_{i_1\,i_2\,i_3}\Big|_{c\ \text{terms}} = \frac{3c}{2}\left[\delta_{i_1\,i_3}\delta_{j_1\,j_2}\delta_{i_2\,j_3}+\delta_{i_1\,i_3}\delta_{i_2\,j_1}\delta_{j_2\,j_3}+\delta_{i_1\,j_2}\delta_{i_2\,j_3}\delta_{i_3\,j_1}+\delta_{i_1\,i_2}\delta_{i_3\,j_1}\delta_{j_2\,j_3}\right] \tag{B.32}$$

and then the matrix element

$$\Gamma_{ss'}(\mathbf{k},\mathbf{k}') = \frac{\hbar}{4\rho_0}\frac{1}{\sqrt{\omega_s(k)\,\omega_{s'}(k')}}\sum_{i_1\,i_2\,i_3}\sum_{j_1\,j_2\,j_3} D^{j_1\,j_2\,j_3}_{i_1\,i_2\,i_3}\, e_{i_1}(\hat{k},s)\, e_{i_2}(\hat{k}',s')\, k_{j_1}\, k'_{j_2}\, \tilde{d}_{i_3 j_3} \tag{B.33}$$

has the contribution from the c terms in (B.31) and (B.32)

$$\Gamma_{ss'}(\mathbf{k},\mathbf{k}')\Big|_{c\,\text{terms}} = \frac{3c\hbar}{8\rho_0}\frac{1}{\sqrt{\omega_s(k)\,\omega_{s'}(k')}}\sum_{i\,j\,l\,m} e_i(\hat{k},s)\, e_j(\hat{k}',s')\,\tilde{d}_{lm}\, t_{ijlm} \tag{B.34}$$

where

$$t_{ijlm}(\mathbf{k},\mathbf{k}') \equiv \delta_{il}\,(\delta_{jm}\,\mathbf{k}\cdot\mathbf{k}' + k_j\,k'_m) + k_l\,(\delta_{jm}\,k'_i + \delta_{ij}\,k'_m) \tag{B.35}$$

after relabelling summation indices. Squaring this and summing over the polarization indices s, s' for the two transverse phonon polarization states for which

$$\sum_{s=T_1,T_2} e_{i_1}(\hat{k},s)\, e_{i_2}(\hat{k},s) = \delta_{i_1 i_2} - \hat{k}_{i_1}\hat{k}_{i_2} \equiv \pi_{i_1 i_2}(\hat{k}) \tag{B.36}$$

is the projector transverse to the direction of propagation $\mathbf{k}$, we obtain

$$\begin{aligned}\sum_{ss'=T_1,T_2}|\Gamma_{ss'}(\mathbf{k},\mathbf{k}')|^2\Big|_{c\,\text{terms}} &= \frac{9c^2\hbar^2}{64\rho_0^2}\frac{1}{\omega(k)\omega(k')}\sum_{i_1 j_1 l_1 m_1}\sum_{i_2 j_2 l_2 m_2}\pi_{i_1 i_2}(\hat{k})\pi_{j_1 j_2}(\hat{k}')\,\tilde{d}_{l_1 m_1}\,\tilde{d}^*_{l_2 m_2}\times \\ &\times\; t_{i_1 j_1 l_1 m_1} t_{i_2 j_2 l_2 m_2}\,.\end{aligned} \tag{B.37}$$

If we evaluate this expression for the screw dislocation which is dominated by its $\tilde{d}_{zx}$ term, we see that the proportionality factor missing in (B.10) is

$$\mathcal{P}\Big|_{c\ \text{terms}} = \frac{9c^2\hbar^2}{64\,\rho_0^2}\sum_{i_1 j_1 i_2 j_2}\pi_{i_1 i_2}(\hat{k})\,\pi_{j_1 j_2}(\hat{k}')\,t_{i_1 j_1 z x}\,t_{i_2 j_2 z x} \tag{B.38}$$

where from (B.35)

$$t_{ijzx} = \delta_{iz}\,(\delta_{jx}\,\mathbf{k}\cdot\mathbf{k}' + k_j\,k'_x) + k_z\,(\delta_{jx}\,k'_i + \delta_{ij}\,k'_x) \tag{B.39}$$

and of course we must substitute for $\mathbf{k}' = \mathbf{k}+\mathbf{q}$ and k_z inside the integral (B.7) using the δ-function constraints (B.2) and (B.8) of momentum and energy conservation.

Now the question relevant to our previous analysis of possible infrared divergences found tentatively in (B.28) in the integral for drag coefficient for screw dislocations due to transverse phonon wind — previously ignoring the direction dependent factor (B.38) — is how is the

conclusion changed when this factor is taken account of. Since t_{ijzx} contains 4 terms and its square appearing in (B.38) is symmetric, we obtain 10 terms from (B.38), which written out explicitly are

$$\sum_{i_1j_1i_2j_2} \pi_{i_1i_2}(\hat{k})\,\pi_{j_1j_2}(\hat{k}')\,t_{i_1j_1zx}\,t_{i_2j_2zx} = \pi_{zz}(\hat{k})\,\pi_{xx}(\hat{k}')\,(\mathbf{k}\cdot\mathbf{k}')^2 +$$
$$+\ 2\,\pi_{zz}(\hat{k})\,\pi_{xj}(\hat{k}')k_j\,(\mathbf{k}\cdot\mathbf{k}')\,k'_x + 2\,k_z\pi_{zi}(\hat{k})k'_i\,\pi_{xx}(\hat{k}')\,(\mathbf{k}\cdot\mathbf{k}') + 2\,\pi_{zi}(\hat{k})\,\pi_{ix}(\hat{k}')\,k_z\,k'_x(\mathbf{k}\cdot\mathbf{k}') +$$
$$+\ \pi_{zz}(\hat{k})\,k_i\pi_{ij}(\hat{k}')k_j\,(k'_x)^2 + 2\,\pi_{zi}(\hat{k})k'_i\,k_j\pi_{jx}(\hat{k}')\,k'_x\,k_z + 2\,\pi_{zi}(\hat{k})\,\pi_{ij}(\hat{k}')k_j\,k_z\,(k'_x)^2 +$$
$$+\ k_z^2k'_i\,\pi_{ij}(\hat{k})k'_j\,\pi_{xx}(\hat{k}') + 4\,k_z^2\,k'_x\,k'_i\,\pi_{ix}(\hat{k})k'_j + 4k_z^2\,(k'_x)^2 \tag{B.40}$$

where

$$\delta_{i_1i_2}\,\pi_{i_1i_2}(\hat{k}) = 2 \tag{B.41}$$

has been used. Each of these 10 terms contains at least two powers of k_z, k_y, k'_y. To see this one has to consider the 10 terms one by one and use

$$\pi_{zz}(\hat{k}) = 1 - \frac{k_z^2}{k_x^2+k_y^2+k_z^2} \to 1 - \frac{k_z^2}{k_x^2} \to 1 \tag{B.42a}$$

$$\pi_{zz}(\hat{k}') = 1 - \frac{k_x'^2}{k_x'^2+k_y'^2+k_z^2} \to \frac{k_y'^2+k_z^2}{k_x^2} \tag{B.42b}$$

$$\pi_{xj}(\hat{k}')k_j = k_x - \frac{k'_x(\mathbf{k}\cdot\mathbf{k}')}{k_x'^2+k_y'^2+k_z^2} \to \frac{k_x(k_y'^2+k_z^2) - k'_x(k_yk'_y+k_z^2)}{k_x'^2} \tag{B.42c}$$

$$k_i\pi_{ij}(\hat{k}')k_j = |\mathbf{k}|^2 - \frac{(\mathbf{k}\cdot\mathbf{k}')^2}{|\mathbf{k}'|^2} \to \frac{k_x^2(k_y'^2+k_z^2) + k_x'^2(k_y^2+k_z^2) - 2k_xk'_x(k_yk'_y+k_z^2)}{k_x^2k_x'^2} \tag{B.42d}$$

$$\pi_{zi}(\hat{k})\,\pi_{ij}(\hat{k}')k_j\,k_z\,(k'_x)^2 = k_z^2\,(k'_x)^2\,\frac{\mathbf{k}\cdot\mathbf{k}'}{|\mathbf{k}'|^2}\left[\frac{\mathbf{k}\cdot\mathbf{k}'}{|\mathbf{k}|^2} - 1\right] \to k_z^2\,k'_x\,(k'_x - k_x) \tag{B.42e}$$

evaluated to leading order in terms quadratic in k_z, k_y, k'_y assumed small compared to $k_x^2, k_x'^2$ since this is what was assumed in evaluating (B.28) without the polynomial (B.38).

Thus this explicit evaluation of the polynomial factor (B.38) left out of the integral (B.28) for the drag coefficient of a screw dislocation due to transverse phonon wind shows that at least two powers of the momentum components assumed small in evaluating (B.28), and which led to its infrared divergence at $v = c_{\rm T}$ are in fact removed when the correct polynomial factor is taken account of. This means that the true expression with all factors taken account of has no infrared divergence and one should *not* assume that components k_z, k_y, k'_y are small in magnitude compared to k_x, k'_x, and in fact all components appear with positive powers in the full expression for the drag coefficients, so that all the momenta are of order of the Debye cutoff momentum $q_{\rm BZ}$, with the finite estimate (B.30) for the final result of the drag coefficient of a screw dislocation due to transverse phonon wind in the limit that its velocity approaches the transverse phonon sound speed $c_{\rm T}$.

B.2 Edge Dislocations Interacting with Transverse Phonons

In the case of the edge dislocation and again concentrating on the transverse phonon wind, a more tedious but straightforward calculation shows that the polynomial direction-dependent factor again contains two powers of the momentum components that tend to suppress the infrared

divergence. But the edge dislocation itself has two extra powers of these small momentum components in the denominator so that the result remains infrared divergent in the limit $v \to c_{\mathrm{T}}$, its degree of divergence being $1/(1-\beta_{\mathrm{T}}^2)^{1/2}$ for edge dislocations.

B.3 Fitting functions

Based on the present analysis at high velocity together with the small velocity limit discussed in Section 5, we expect good fits over the range we computed using

$$\begin{aligned} B^{\mathrm{edge}} &\approx C_0^{\mathrm{e}} + C_1^{\mathrm{e}}\beta_{\mathrm{T}} + C_2^{\mathrm{e}}\beta_{\mathrm{T}}^2 + C_3^{\mathrm{e}}\log\left(1-\beta_{\mathrm{T}}^2\right) + C_4^{\mathrm{e}}\left(\frac{1}{\sqrt{1-\beta_{\mathrm{T}}^2}} - 1\right) , \\ B^{\mathrm{screw}} &\approx C_0^{\mathrm{s}} + C_1^{\mathrm{s}}\beta_{\mathrm{T}} + C_2^{\mathrm{s}}\beta_{\mathrm{T}}^2 + C_3^{\mathrm{s}}\beta_{\mathrm{T}}^4 + C_4^{\mathrm{s}}\beta_{\mathrm{T}}^{16} . \end{aligned} \tag{B.43}$$

The divergent terms are motivated by the present analysis, and the polynomial terms are needed to get good agreement in the small velocity regime. From (5.3) we know that the next to leading order term in the small velocity expansion is quadratic in the velocity (which is also why we need β_{T}^2 in the pole terms), and since there is no divergent term in the screw case, we required an additional β_{T}^8 term in order to increase the accuracy of the fit. This latter step was validated using the numerical results of Section 5. The relations between the β_{T}^2, β_{T}^4, and β_{T}^6 terms were determined empirically as well.

References

[1] A. Hunter and D. L. Preston, "Analytic model of the remobilization of pinned glide dislocations from quasi-static to high strain rates", *Int. J. Plast.* **70** (2015) 1–29.

[2] E. M. Nadgornyi, "Dislocation dynamics and mechanical properties of crystals", *Prog. Mater. Sci.* **31** (1988) 1–530.

[3] P. Rosakis, "Supersonic dislocation kinetics from an augmented Peierls model", *Phys. Rev. Lett.* **86** (2001) 95–98.

[4] V. Nosenko, S. Zhdanov, and G. Morfill, "Supersonic dislocations observed in a plasma crystal", *Phys. Rev. Lett.* **99** (2007) 025002, arXiv:0709.1782 [cond-mat.soft].

[5] Y.-P. Pellegrini, "Dynamic Peierls-Nabarro equations for elastically isotropic crystals", *Phys. Rev.* **B81** (2010) 024101, arXiv:0908.2371 [cond-mat.mtrl-sci].

[6] C. J. Ruestes, E. M. Bringa, R. E. Rudd, B. A. Remington, T. P. Remington, and M. A. Meyers, "Probing the character of ultra-fast dislocations", *Sci. Rep.* **5** (2015) 16892.

[7] D. C. Wallace, *Thermodynamics of Crystals*, (New York: J. Wiley & Sons Inc., 1972).

[8] J. D. Eshelby, "Uniformly moving dislocations", *Proc. Phys. Soc.* **A62** (1949) 307.

[9] J. Weertman and J. R. Weertman, "Moving dislocations", in *Moving Dislocations*, F. R. N. Nabarro, ed., vol. 3 of *Dislocations in Solids*, pp. 1–59, (Amsterdam: North Holland Pub. Co., 1980).

[10] L. Landau and E. Lifshitz, *Theory of Elasticity*, third ed., vol. 7 of *Course of Theoretical Physics*, (Butterworth-Heinemann, 1986).

[11] J. P. Hirth and J. Lothe, *Theory of Dislocations*, second ed., (New York: Wiley, 1982).

[12] F. D. Murnaghan, "Finite deformations of an elastic solid", *Am. J. Math* **59** (1937) 235–260.

[13] J. Lubliner, *Plasticity Theory*, Dover ed., Dover Books on Engineering, (Dover, 2008).

[14] R. A. Toupin and B. Bernstein, "Sound waves in deformed perfectly elastic materials. Acoustoelastic effect", *J. Acoust. Soc. Am.* **33** (1961) 216–225.

[15] A. D. Volkov, A. I. Kokshaiskii, A. I. Korobov, and V. M. Prokhorov, "Second- and third-order elastic coefficients in polycrystalline aluminum alloy AMg6", *Acoust. Phys.* **61** (2015) 651–656.

[16] D. C. Wallace, "Thermoelastic theory of stressed crystals and higher-order elastic constants", in vol. 25 of *Solid State Physics*, pp. 301–404, H. Ehrenreich, F. Seitz, and D. Turnbill, eds., (New York: Academic Press, 1970).

[17] V. A. Lubarda, "New estimates of the third-order elastic constants for isotropic aggregates of cubic crystals", *J. Mech. Phys. Solids* **45** (1997) 471–490.

[18] D. N. Blaschke, "Averaging of elastic constants for polycrystals", *J. Appl. Phys.* **122** (2017) 145110, arXiv:1706.07132 [cond-mat.mtrl-sci].

[19] J. M. Burgers, "Some considerations on the fields of stress connected with dislocations in a regular crystal lattice. I", *Proc. Kon. Ned. Akad. v. Wet.* **42** (1939) 293–325.

[20] J. Weertman, "High velocity dislocations", in *Response of Metals to High Velocity Deformation*, P. G. Shewmon and V. F. Zackay, eds., vol. 9 of *Metallurgical Society Conferences*, pp. 205–247, (New York: Interscience Publishers, 1961). Proc. of a technical conference, Estes Park, Colorado, 1960.

[21] V. I. Alshits, "The phonon-dislocation interaction and its role in dislocation dragging and thermal resistivity", in *Elastic Strain Fields and Dislocation Mobility*, V. L. Indenbom and J. Lothe, eds., vol. 31 of *Modern Problems in Condensed Matter Sciences*, pp. 625–697, (Elsevier, 1992).

[22] V. I. Al'shits, M. D. Mitlianskij, and R. K. Kotowski, "The phonon wind as a non-linear mechanism of dislocation dragging", *Arch. Mech.* **31** (1979) 91–105.

[23] V. I. Al'shits, "Raman scattering of phonons as a cause of dislocation damping", *Sov. Phys. Solid State* **11** (1969) 1081–1087, [*Fiz. Tverd. Tela* **11** (1969) 1336–1344].

[24] V. I. Al'shits, "'Phonon wind' and dislocation damping", *Sov. Phys. Solid State* **11** (1970) 1947–1948, [*Fiz. Tverd. Tela* **11** (1969) 2405–2407].

[25] V. I. Al'shitz and A. G. Mal'shukov, "Phonon component of dynamic dragging of dislocations", *Sov. Phys. JETP* **36** (1973) 978–982, [*Zh. Eksp. Teor. Fiz.* **63** (1972) 1849–1857].

[26] A. D. Brailsford, "Anharmonicity contributions to dislocation drag", *J. Appl. Phys.* **43** (1972) 1380–1393.

[27] G. Grimvall, *Thermophysical Properties of Materials*, enlarged and revised ed., (Amsterdam: Elsevier Science B.V., 1999).

[28] V. A. Al'shitz and V. L. Indenbom, "Dynamic dragging of dislocations", *Sov. Phys. Usp.* **18** (1975) 1–20, [*Usp. Fiz. Nauk.* **115** (1975) 3–39].

[29] M. Abramowitz and I. A. Stegun, eds., *Handbook of Mathematical Functions with Formulas, Graphs, and Mathematical Tables*, 10th ed., vol. 55 of *Applied Mathematics Series*, (Nat. Bur. Stand. (U.S.), 1972).

[30] P. Debye, "Zur Theorie der spezifischen Wärmen", *Annalen Phys.* **344** (1912) 789–839.

[31] J. Marian and A. Caro, "Moving dislocations in disordered alloys: Connecting continuum and discrete models with atomistic simulations", *Phys. Rev.* **B74** (2006) 024113.

[32] E. Oren, E. Yahel, and G. Makov, "Dislocation kinematics: a molecular dynamics study in Cu", *Mod. Simul. Mater. Sci. Eng.* **25** (2017) 025002.

[33] D. N. Blaschke and B. A. Szajewski, "Line tension of a dislocation moving through an anisotropic crystal", arXiv:1711.10555 [cond-mat.mtrl-sci].

[34] V. S. Krasnikov, A. Yu. Kuksin, A. E. Mayer, and A. V. Yanilkin, "Plastic deformation under high-rate loading: The multiscale approach", *Phys. Solid State* **52** (2010) 1386–1396.

[35] A. Seeger and O. Buck, "Die experimentelle Ermittlung der elastischen Konstanten höherer Ordnung", *Z. Naturf.* **15a** (1960) 1056–1067.

[36] W. Wasserbäch, "Third-order constants of a cubic quasi-isotropic solid", *phys. stat. sol. (b)* **159** (1990) 689–697.

[37] W. M. Haynes, *CRC Handbook of Chemistry and Physics*, 97th ed., (CRC Press, 2017).

[38] R. W. Hertzberg, R. P. Vinci, and J. L. Hertzberg, *Deformation and Fracture Mechanics of Engineering Materials*, fifth ed., (Wiley, 2012).

[39] L. J. Graham, H. Nadler, and R. Chang, "Third-order elastic constants of single-crystal and polycrystalline columbium", *J. Appl. Phys.* **39** (1968) 3025–3033.

[40] F. C. Frank, "Dislocation theory", *Nuov. Cim.* **7** (1958) 386–413.

[41] J. Cotner and J. Weertman, "High dislocation velocities and the structures of slip bands in shock loaded high purity lithium fluoride", *Discuss. Faraday Soc.* **38** (1964) 225–232.

[42] E. V. Darinskaya, I. P. Makarevich, Yu. I. Meshcheryakov, V. A. Morozov, and A. A. Urusovskaya, "Investigation of the mobility of edge dislocations in LiF and NaCl crystals subjected to pulse loading with an electron beam", *Sov. Phys. Solid State* **24** (1982) 898, [*Fiz. Tverd. Tela* **24** (1982) 1564].

[43] J. A. Gorman, D. S. Wood, and T. Vreeland Jr., "Mobility of dislocations in aluminum", *J. Appl. Phys.* **40** (1969) 833–841.

[44] V. R. Parameswaran, N. Urabe, and J. Weertman, "Dislocation mobility in aluminum", *J. Appl. Phys.* **43** (1972) 2982–2986.

[45] D. L. Olmsted, L. G. Hector Jr., W. A. Curtin, and R. J. Clifton, "Atomistic simulations of dislocation mobility in Al, Ni and Al/Mg alloys", *Mod. Simul. Mater. Sci. Eng.* **13** (2005) 371, `arXiv:cond-mat/0412324`.

[46] T. Suzuki, A. Ikushima, and M. Aoki, "Acoustic attenuation studies of the frictional force on a fast moving dislocation", *Acta Met.* **12** (1964) 1231–1240.

[47] K. M. Jassby and T. Vreeland Jr., "Dislocation mobility in pure copper at 4.2°K", *Phys. Rev.* **B8** (1973) 3537–3541.

[48] E. B. Zaretsky and G. I. Kanel, "Response of copper to shock-wave loading at temperatures up to the melting point", *J. Appl. Phys.* **114** (2013) 083511.

[49] R. M. Stern and A. V. Granato, "Overdamped resonance of dislocations in copper", *Acta Met.* **10** (1962) 358–381.

[50] W. F. Greenman, T. Vreeland Jr., and D. S. Wood, "Dislocation mobility in copper", *J. Appl. Phys.* **38** (1967) 3595–3603.

[51] G. A. Alers and D. O. Thompson, "Dislocation contributions to the modulus and damping in copper at megacycle frequencies", *J. Appl. Phys.* **32** (1961) 283–293.

[52] N. Urabe and J. Weertman, "Dislocation mobility in potassium and iron single crystals", *Mater. Sci. Eng.* **18** (1975) 41–49.

[53] M. R. Gilbert, S. Queyreau, and J. Marian, "Stress and temperature dependence of screw dislocation mobility in α-Fe by molecular dynamics", *Phys. Rev.* **B84** (2011) 174103.

[54] D. L. Preston and D. C. Wallace, "A model of the shear modulus", *Solid State Commun.* **81** (1992) 277–281.

[55] L. Burakovsky, C. W. Greeff, and D. L. Preston, "Analytic model of the shear modulus at all temperatures and densities", *Phys. Rev.* **B67** (2003) 094107, `arXiv:cond-mat/0208585`.

[56] I. S. Gradshteyn and I. M. Ryzhik, *Table of Integrals, Series and Products*, seventh ed., A. Jeffrey and D. Zwillinger, eds., (Academic Press, 2007).

[57] L. Burakovsky, D. L. Preston, and R. R. Silbar, "Melting as a dislocation-mediated phase transition", *Phys. Rev.* **B61** (2000) 15011–15018, `arXiv:cond-mat/0004011`.